A generalized model of pelagic biogeochemistry for the global ocean ecosystem. Part I: theory.

M. Vichi [a,*] N. Pinardi [b] S. Masina [a]

[a] *Istituto Nazionale di Geofisica e Vulcanologia, Sezione di Bologna, Italy*

[b] *Alma Mater Studiorum Università di Bologna, Centro Interdipartimentale per la Ricerca sulle Scienze Ambientali, Ravenna, Italy*

Abstract

The set of equations for global ocean biogeochemistry deterministic models have been formulated in a comprehensive and unified form in order to use them in numerical simulations of the marine ecosystem for climate change studies (PELAGOS, PELAgic biogeochemistry for Global Ocean Simulations). The fundamental approach stems from the representation of marine trophic interactions and major biogeochemical cycles introduced in the European Regional Seas Ecosystem Model (ERSEM). Our theoretical formulation revisits and generalizes the stoichiometric approach of ERSEM by defining the state variables as Chemical Functional Families (CFF). CFFs are further subdivided into living, non-living and inorganic components. Living CFFs are the basis for the definition of Living Functional Groups, the biomass-based functional prototype of the real organisms. Both CFFs and LFGs are theoretical constructs which allow us to relate measurable properties of marine biogeochemistry to the state variables used in deterministic models. This approach is sufficiently generic that may be used to describe other existing biomass-based ecosystem model.

Key words: marine biogeochemistry, biomass-based ecosystem model, ecological stoichiometry, ERSEM, PELAGOS, BFM

1 Introduction

Biogeochemical models representing trophic and chemical interactions in the marine system have been discussed largely in the past 20 years (see reviews by Hof-

* Corresponding author. Address: INGV, Sezione di Bologna, V. Creti 12, 40128 Bologna. Tel: +39 051 4151 456 Fax: +39 051 4151 499
Email address: vichi@bo.ingv.it (M. Vichi).

mann and Lascara, 1998; McCarthy et al., 2002; Denman, 2003), particularly focusing on a biomass-based description of the pelagic system. Nevertheless, a theoretical formulation of the basic equations in terms of partial differential equations (pde) of key biogeochemical constituents and associated rates has not been published yet in the scientific literature. This kind of approach helps to define the numerical implementation of marine biogeochemistry coupled with physical circulation models at all spatial and temporal scales.

The aim of this paper is to formulate a set of equations describing the pelagic biogeochemistry coupled to physical processes of importance. We call this a generalized model of pelagic biogeochemistry, meaning the mathematical representation, by means of partial differential equations of biogeochemical processes. In general the pdes contain the divergence of material fluxes that determine the rate of change of the ecosystem state variables.

The biogeochemical rates of change are outlined starting from the parameterizations of the European Regional Seas Ecosystem Model (Baretta et al., 1995; Baretta-Bekker et al., 1997, ERSEM I and ERSEM II), which was the first comprehensive ecosystem model to include physiological considerations in the definition of the divergence of material fluxes. However, in the original ERSEM papers (Baretta et al., 1995; Baretta-Bekker et al., 1997, and other papers in the two special issues), the biogeochemical process formulations were given in a finite difference form, and a general formalism of pdes was actually lacking.

On the other hand several implementations of this model have shown the skill of this approach, both in coastal areas with large land-derived inputs but also in the oligotrophic Mediterranean regions and in the subtropical Atlantic Ocean (Ruardij et al., 1997; Allen et al., 1998; Vichi et al., 1998; Zavatarelli et al., 2000; Obernosterer et al., 2001; Allen et al., 2001; Petihakis et al., 2002; Vichi et al., 2004; Raick et al., 2005). The same approach has also been used in the context of climate studies, particularly to capture and analyze climate variability in the North Sea and in the Adriatic Sea (Taylor et al., 2002; Vichi et al., 2003a). A direct descendant of ERSEM, the Biogeochemical Flux Model (BFM), is now being developed in the framework of the EU project MFSTEP (Mediterranean Forecasting System Toward Environmental Predictions, http://www.bo.ingv.it/mfstep) and applied to the whole Mediterranean basin and subregional seas. Finally, a recent publication (Blackford et al., 2004) has shown that the ERSEM approach to pelagic biogeochemistry was able to adapt to contrasting sites in the world ocean making it appealing for applications in the global ocean.

In this paper we present the pde formulation of pelagic biogeochemistry in a general framework. As recently stated by Anderson (2005), the continued articulation of details in ecosystem models needs to be pursued with due care and attention to the formulations employed, and therefore a common unified formalism is necessary. Our aim is to generalize the biogeochemical concepts developed in ERSEM

beyond their original implementation in coastal ecosystems. We do that elucidating the basic constituents and introducing a clear definition of the ecosystem state variables that may be further generalized to include more processes if needed. Particularly, our equations are different from ERSEM for the addition of important biogeochemical constituents such as iron and chlorophyll which are relevant for global ocean biogeochemistry.

We propose a new nomenclature and formalism which highlight the general concepts behind the biomass approach to marine biogeochemistry. We also formalize the definition and grouping of model state variables and interactions, which helps to understand the basic model hypotheses and assumptions. A companion paper (Vichi et al., 2006) presents the numerical implementation of this revised model to the global ocean ecosystem with a direct coupling to a general circulation model, and a comparison with the distribution and seasonal variability of bulk properties (nutrients and satellite chlorophyll) and the different phytoplankton groups.

The paper is organized as follows. In Section 2 we give an overview of the theoretical approach and the basic equations describing the pelagic biogeochemical processes. In Section 3 we illustrate the basic formalism and nomenclature used throughout the paper. Section 4 presents the physical parameters that affect pelagic biogeochemistry. In Section 5 the biogeochemical equations are written in all details for the pelagic state variables and Section 6 offers a discussion.

2 Towards a generic formalism for pelagic biogeochemistry

The ERSEM view of the marine ecosystem was based upon the recognition that the major ecological functions of producers, decomposers and consumers and their specific trophic interactions can be expressed in terms of material flows of basic elements (C, N, P, etc.). The concentration and characteristics of organic and inorganic species in the water were thus seen under a stoichiometrical perspective as the final result of the direct uptake and release by producers, decomposers, heterotrophic consumers of these constituents. The central role was thus not played by single species but by the total biomass of a collection of species sharing the same functional behavior.

This functional approach is rewritten here with a new formalism which is based on the definition of Chemical Functional Families (CFF) and Living Functional Groups (LFG). The core components of the formalism are the CFFs (Fig. 1) which are theoretical constructs that are useful to describe the way materials are exchanged in marine biogeochemistry. CFFs can be sometimes identified as specific compounds such as dissolved inorganic nutrients, but in most of the cases are defined as the inventory of a certain biogeochemical element contained in more complex living and non-living components of marine biogeochemical cycles. A typical

example is the total C content in phytoplankton or bacteria and N content in dissolved or particulate organic matter. CFFs can be described in terms of concentrations and the choice of CFFs as the basic state variables is natural since they are measurable quantities in the limits of laboratory or in situ experiments. CFFs are divided in inorganic, non-living organic and living organic compounds (Fig. 1) and they are measured in equivalents of major chemical elements (C, N, P, Si, O, Fe) or in molecular weight units as in the case of chlorophyll. Their type and number cannot be fixed a priori and it is mostly linked to the degree of knowledge of the relevant biogeochemical processes.

The concept of LFG is more familiar, and has been frequently used in marine and terrestrial ecosystem modelling (Baretta and Ruardij, 1988; Smith et al., 1997; Le Quéré et al., 2005). Producers, consumers and decomposers are broad LFGs, and further criteria can be defined for further distinguishing assemblages of organisms that have an explicit biogeochemical role in marine ecosystems (Le Quéré et al., 2005). In the pelagic domain, the term LFG is equivalent to Plankton Functional Type (PFT Le Quéré et al., 2005; Anderson, 2005). However, aiming at a more generalized approach, LFG is preferable because allows to include other functional groups which are not planktonic, such as benthic organisms or any possible biomass-based representation of fish.

Members of one LFG are represented by the prototype of a standard organism as in Fig. 2 (modified after Baretta et al., 1995). As well as CFFs, also the standard organism is a theoretical construct, which should not be identified with the real organism. The standard organism is thus the model of the LFGs, whose total biomass is composed of living CFFs and interacts with other (living and non-living) CFFs by means of universal physiological and ecological processes such as photosynthesis, excretion, grazing, etc. The parameterization of the physiological and trophic dynamics considered are generally limited to interactions at membrane level, which also implies neglecting the details of ingestion mechanisms in metazoans. It is important to notice that this approach does not exclude the further implementation of more detailed formulations which mechanistically resolve the intracellular transport of nutrients and carbon (e.g. Flynn, 2001) or parameterizations of the feeding behavior of zooplankton.

The mathematical relationships between the CFFs (i.e. the LFG's internal content of C, N, P, etc., Fig. 2) and the LFG functionalities are defined following the stoichiometrical requirements of basic elements. These requirements can be both dynamically varying between given maximum and minimum values of element ratios or constant. This makes the definition of LFGs very general and can be also applied, for instance, to other existing biogeochemical models which use one single nutrient as currency. If it is assumed that the standard organism has fixed stoichiometry (e.g., Redfield ratios in phytoplankton), then the dynamics of the LFG can be formulated with one single CFF, and the time rate of change of the others are derived from the constant ratios.

Starting from the theoretical assumption that the ecosystem can be basically described by concentrations of CFFs in living and non-living components, we can write the conservation equation for an infinitesimal volume of fluid. Here we make again the continuum hypothesis (Batchelor, 1967), i.e., if C_i indicates a given CFF concentration, the values of C_i is a continuous function of space and time. The basic equation in a fluid is thus:

$$\frac{\partial C_i}{\partial t} = -\vec{\nabla} \cdot \vec{F}, \tag{1}$$

where $\vec{F}$ is a generalized flux of C_i through and within the basic infinitesimal element of mass of the fluid. This flux can be further separated in a physical part and a biological reaction term

$$\frac{\partial C_i}{\partial t} = -\vec{\nabla} \cdot \vec{F}_{phys} - \vec{\nabla} \cdot \vec{F}_{bio}. \tag{2}$$

The second term on the right hand side of (2) cannot be measured directly and therefore we assume that it can be approximated in the following way:

$$\vec{\nabla} \cdot \vec{F}_{bio} = -w_B \frac{\partial C_i}{\partial z} + \left.\frac{\partial C_i}{\partial t}\right|_{bio}. \tag{3}$$

Both terms in eq. (4) represent the biogeochemical divergence flux and parameterize the sinking of biological particulate matter and the local time rate of change due to biogeochemical transformation processes. The sinking velocity w_B is introduced for those state variables that have a distinctive vertical velocity with respect to fluid vertical velocity.

This approximation brings us to the well-known form of an advection-diffusion-reaction equation in a moving ocean:

$$\frac{\partial C_i}{\partial t} = -\nabla \cdot (\mathbf{u} C_i) + \nabla_H \cdot (A_H \nabla_H C_i) + \frac{\partial}{\partial z} A_V \frac{\partial C_i}{\partial z} - w_B \frac{\partial C_i}{\partial z} + \left.\frac{\partial C_i}{\partial t}\right|_{bio} \tag{4}$$

where $\mathbf{u} \equiv (u, v, w)$ is the three-dimensional current velocity and (A_H, A_V) are the turbulent diffusivity coefficients.

The primitive form (4) is at the basis of biomass-based ecosystem modelling in the ocean (e.g. Hofmann and Lascara, 1998). Our model starts from these assumptions trying to identify the most complete formulation of the biological rate term in (3) for the different CFF state variables listed in Tab. 1. We write here the equations for this term building on the ERSEM approach, somewhat following the original notation (Blackford and Radford, 1995) but upgrading it for the definition of state variables and rates of change. As shown in Tab. 1, each LFG is mathematically expressed by a multi-dimensional array that contains the concentrations of the living CFF based upon the biogeochemical elements. We use a superscript indicating

the CFF for a specific living functional group and a subscript for the basic constituent. For instance, diatoms are LFG of producers and comprise 6 living CFFs written as $P_i^{(1)} \equiv \left(P_c^{(1)}, P_n^{(1)}, P_p^{(1)}, P_s^{(1)}, P_f^{(1)}, P_l^{(1)}\right)$ for the C, N, P, Si, Fe and chlorophyll content; particulate organic detritus is composed of 5 non-living CFFs as $R_i^{(6)} \equiv \left(R_c^{(6)}, R_n^{(6)}, R_p^{(6)}, R_s^{(6)}, R_f^{(6)}\right)$.

The particular configuration of 44 CFF state variables shown in Fig. 3 was chosen for testing in a global ocean coupled physical-biogeochemical numerical application named PELAGOS (PELAgic biogeochemistry model for Global Ocean Simulations), which is fully presented in the companion paper (Vichi et al., 2006, submitted). The model resolves 3 different LFGs for phytoplankton $P^{(j)}$, $j = 1,2,3$ (diatoms, autotrophic nanoflagellates and picophytoplankton), 3 for zooplankton $Z^{(j)}$, $j = 4,5,6$ (omnivorous mesozooplankton, microzooplankton and heterotrophic nanoflagellates), 1 LFG for bacteria, 8 inorganic CFFs for nutrients and gases (phosphate, nitrate, ammonium, silicate, dissolved iron, reduction equivalents, oxygen, carbon dioxide) and 8 organic non-living CFFs for dissolved and particulate detritus (cfr. Tab. 1 and Fig. 3). The state variable nitrate is assumed here to be the sum of both nitrate and nitrite. Reduction equivalents represent all the reduced ions produced under anaerobic conditions. This variable was originally used only in the benthic nutrient regeneration module of ERSEM (Ruardij and Van Raaphorst, 1995) but was extended to the water column in Vichi et al. (2004).

With this kind of approach, all the nutrient:carbon ratios in chemical organic and living functional groups are allowed to vary within their given ranges and each component has a distinct biological time rate of change. This kind of parameterizations are meant to mimic the adaptation of organisms to the diverse availability of nutrients and light observed in the world ocean, and also allow to recycle organic matter along the water column depending on the actual nutrient content (Baretta et al., 1995; Vichi et al., 2003b; Polimene et al., 2006).

3 The basic formalism of the biological rate term

Each state variable interacts with the others through the universal physiological and ecological processes depicted in Fig. 3, which are mostly derived from the original ERSEM scheme (Baretta et al., 1995). The biological reaction term in eq. (4) is generally written in ecological modelling as an ordinary differential equation holding the primitive biogeochemical processes on the right hand side. For a generic phytoplankton state variables P, for instance, the biological term is indicated as:

$$\frac{dP}{dt} = \text{Uptake} - \text{Exudation} - \text{Lysis} - \text{Respiration} - \text{Grazing}$$

On the other hand, for a generic Z state variable of mesozooplankton, the reaction term is composed of the following processes:

$$\frac{dZ}{dt} = \text{Ingestion} - \text{Egestion} - \text{Respiration} - \text{Predation}$$

A generic B state variable for bacteria has a reaction term written as:

$$\frac{dB}{dt} = \text{Uptake} - \text{Remineralization} - \text{Respiration} - \text{Predation}$$

The terms for the inorganic and organic components are eventually derived from the relations above using conservation principles. This kind of notation is used in the scientific literature and is meant to emphasize the zero-dimensional biological interactions shown in Fig. 3. However, it can hardly be generalized in mathematical terms and at any spatial scale and therefore a pde form is preferable. We use here two different interpretation levels: 1) rates of change form; and 2) explicit functional form. In "rates of change form", the biogeochemical reaction term in (4) for the CFF state variable C is written as:

$$\left.\frac{\partial C}{\partial t}\right|_{bio} = \sum_{i=1,n} \sum_{j=1,m} \left.\frac{\partial C}{\partial t}\right|_{V_i}^{e_j}, \tag{5}$$

where the right hand side contains the terms representing significant processes for each living or non-living CFF. The superscripts e_j are the abbreviations indicating the process which determines the variation. In Table 2 we report the acronyms of the processes used in the superscripts. The subscripts V_i is the CFF state variable involved in the process. If $V = C$, we refer to intra-group interactions such as cannibalism.

When a term is present as a source in one equation and as a sink in another, we refer to it following this equivalent notation:

$$\left.\frac{\partial C}{\partial t}\right|_{V}^{e} = - \left.\frac{\partial V}{\partial t}\right|_{C}^{e}. \tag{6}$$

In "functional process form", the formulation of the dynamic dependencies on other variables is made explicit, *i.e.*: all the rates of change in (5) are given in the complete functional parameterization. Although this is the more complete mathematical form, it is more difficult to read and interpret at a glance, especially when trying to distinguish which processes affect which variable dynamics. Thus, in our description, we will write the equations both in rate of change and in functional process forms.

4 The environmental parameters affecting biological rates

Before starting with the model equations in their full form we describe the dependencies of the biogeochemical processes from the physical environment. In eq. (4) the coupling between physics and biogeochemistry is realized explicitly through the advecting velocity field and the diffusion coefficients. There is another implicit coupling which affects the biological reaction term through surface irradiance and temperature that are also provided by the physical model. Temperature regulates several physiological processes in the model and its effect, denoted by f^T, is parameterized in this non-dimensional form

$$f^T = Q_{10}^{\frac{T-10}{10}} \tag{7}$$

where the Q_{10} coefficient is different for each functional process considered (see Appendix).

Light is fundamental for primary producers and the energy source for photosynthesis is the underwater transmitted amount of the incident solar radiation at the sea surface. We assume that the Photosynthetic Available Radiation (PAR) E_{PAR} (the notation of Sakshaug et al., 1997, is used here) is parameterized according to the Lambert-Beer formulation with depth-dependent extinction coefficients

$$E_{PAR}(z) = \varepsilon_{PAR}\, Q_S\, e^{\lambda_w z + \int_z^0 \lambda_{bio}(z')dz'} \tag{8}$$

The short-wave surface irradiance flux Q_S is obtained generally from an atmospheric radiative transfer model and is converted from W m^{-2} to the units of μE m^{-2} $s^{-1}$with the constant factor 1/0.215 (Reinart et al., 1998). ε_{PAR} is the coefficient determining the portion of PAR in Q_S. Light propagation takes into account the extinction due to suspended particles, λ_{bio}, and λ_w as the background extinction of water. The biological extinction is written as

$$\lambda_{bio} = \sum_{j=1}^{3} c_{P(j)} P_l^{(j)} + c_{R^{(6)}} R_c^{(6)} \tag{9}$$

where the extinctions due to the concentration of phytoplankton chlorophyll and particulate detritus are considered. Extinction due to dissolved substances and inorganic suspended matter is currently not considered for global ocean applications. The c constants are the specific absorption coefficients of each suspended substance (see Appendix).

5 The biogeochemical equations

In this section we write the reaction terms for the 44 state variables both in the rates of change and in the explicit functional forms. We group them into the classical ERSEM subdivision of LFGs (phytoplankton, zooplankton and bacteria) and we add the equations for all the CFFs.

5.1 Phytoplankton

The dispute about the number of phytoplankton functional groups to be represented in ecosystem models is still open, but there is some consensus on about 5 distinct types (Le Quéré et al., 2005): siliceous and calcareous autotrophs, autotrophic nanoflagellates (chlorophytes), cyanobacteria and picophytoplankton. The original ERSEM II structure already comprised some of these groups (Baretta-Bekker et al., 1997). In this formulation we decided to leave out large dinoflagellates because they are assumed to be of limited importance in open ocean waters. There are three functional subgroups (Table 1 and Fig. 3): diatoms, autotrophic nanoflagellates, and picophytoplankton. Diatoms ($P_i^{(1)}$ in the model) have an Equivalent Spherical Diameter (ESD) of 20-200 μm, preyed upon by adult mesozooplankton (>200 μm, $Z_i^{(4)}$) and partially by microzooplankton of larger dimensions (20-200 μm, $Z_i^{(5)}$). They are the main source of biogenic silica in the model and differ from the other groups because their growth is limited by dissolved silicate. Flagellates $P_i^{(2)}$, ESD = 2-20 μm (nanoplankton), are mainly preyed by microzooplankton. Picophytoplankton $P_i^{(3)}$ has a nominal ESD of 0.2-2 μm. In a global ocean context, our picophytoplankton represents procaryotic organism generally indicated as non-diazotrophic autotrophic bacteria such as *Prochlorococcus* and *Synechococcus*, but can also include eucaryotic species (Worden et al., 2004). Picophytoplankton have an important ecological role because they are the main sources of carbon for heterotrophic nanoflagellates.

The processes parameterized in the biological source term of eq. (4) are gross primary production (*gpp*), respiration (*rsp*), exudation (*exu*), cell lysis (*lys*), nutrient uptake (*upt*), predation (*prd*) and biochemical synthesis (*syn*). All the phytoplankton groups share the same form of primitive equations, but are differentiated in terms of the values of the physiological parameters (see Appendix for a table of the values). There are 6 living CFFs that describes the constituents of phytoplankton (C, N, P, Si, Fe and Chl) and thus for each group we have 5 or 6 equations:

$$\left.\frac{\partial P_c}{\partial t}\right|_{bio} = \left.\frac{\partial P_c}{\partial t}\right|_{O^{(3)}}^{gpp} - \left.\frac{\partial P_c}{\partial t}\right|_{R_c^{(1)}}^{exu} - \left.\frac{\partial P_c}{\partial t}\right|_{O^{(3)}}^{rsp} - \sum_{j=1,6} \left.\frac{\partial P_c}{\partial t}\right|_{R_c^{(j)}}^{lys} - \sum_{k=4,5,6} \left.\frac{\partial P_c}{\partial t}\right|_{Z_c^{(k)}}^{prd} \quad (10)$$

$$\left.\frac{\partial P_n}{\partial t}\right|_{bio} = \sum_{i=3,4} \left.\frac{\partial P_n}{\partial t}\right|_{N^{(i)}}^{upt} - \sum_{j=1,6} \left.\frac{\partial P_n}{\partial t}\right|_{R_n^{(j)}}^{lys} - \frac{P_n}{P_c} \sum_{k=4,5,6} \left.\frac{\partial P_c}{\partial t}\right|_{Z_c^{(k)}}^{prd} \quad (11)$$

$$\left.\frac{\partial P_p}{\partial t}\right|_{bio} = \left.\frac{\partial P_p}{\partial t}\right|_{N^{(1)}}^{upt} - \sum_{j=1,6} \left.\frac{\partial P_p}{\partial t}\right|_{R_p^{(i)}}^{lys} - \frac{P_p}{P_c} \sum_{k=4,5,6} \left.\frac{\partial P_c}{\partial t}\right|_{Z_c^{(k)}}^{prd} \quad (12)$$

$$\left.\frac{\partial P_s}{\partial t}\right|_{bio} = \left.\frac{\partial P_s}{\partial t}\right|_{N^{(5)}}^{upt} - \left.\frac{\partial P_s}{\partial t}\right|_{R_s^{(6)}}^{lys} - \frac{P_s}{P_c} \sum_{k=4,5,6} \left.\frac{\partial P_c}{\partial t}\right|_{Z_c^{(k)}}^{prd} \quad (13)$$

$$\text{if } P_s = P_s^{(1)}, \text{ otherwise } \left.\frac{\partial P_s}{\partial t}\right|_{bio} = 0$$

$$\left.\frac{\partial P_l}{\partial t}\right|_{bio} = \left.\frac{\partial P_l}{\partial t}\right|^{syn} - \frac{P_l}{P_c} \sum_j \left.\frac{\partial P_c}{\partial t}\right|_{Z_c^{(j)}}^{prd} \quad (14)$$

$$\left.\frac{\partial P_f}{\partial t}\right|_{bio} = \left.\frac{\partial P_f}{\partial t}\right|_{N^{(7)}}^{upt} - \left.\frac{\partial P_f}{\partial t}\right|_{R_f^{(6)}}^{lys} - \frac{P_f}{P_c} \sum_{k=4,5,6} \left.\frac{\partial P_c}{\partial t}\right|_{Z_c^{(k)}}^{prd} \quad (15)$$

Most of the terms in eq. 10-13 have already been described in ERSEM II (Baretta-Bekker et al., 1997). Eq. 14 and 15 are new instead, and will be explained in details below. The predation terms are described in Sec. 5.2 when discussing zooplankton dynamics since they are conversion terms in the notation (6).

5.1.1 Carbon and nutrient dynamics

Gross primary production in eq. (10) is the rate of change of phytoplankton carbon P_c due to photosynthesis that involves an uptake of dissolved carbon dioxide $O^{(3)}$. This term is written as:

$$\left.\frac{\partial P_c}{\partial t}\right|_{O^{(3)}}^{gpp} = f_P^T f_P^E f_P^f f_P^s r_P^0 P_c, \quad (16)$$

where r_P^0 is the maximum specific photosynthetic rate under nutrient-replete, light-saturated conditions, and the f functions are multiplicative, non-dimensional regulating factors for temperature, light, iron and silicate, respectively.

This functional form comes from the original ERSEM parameterization of photosynthesis (Baretta-Bekker et al., 1997; Ebenhöh et al., 1997; Vichi, 2002) and has been modified here according to the notation suggested in Sakshaug et al. (1997). The non-dimensional light regulating factor is rewritten from the Webb et al. (1974)

or Platt et al. (1980) formulation (without considering photoinhibition) as:

$$f_P^E = 1 - \exp\left(-\frac{E_{PAR}}{E_K}\right) \tag{17}$$

where E_{PAR} is the available light and E_K the light saturation parameter, which corresponds to the variable I_{opt} in the original ERSEM formulation (Ebenhöh et al., 1997). According to the Sakshaug et al. (1997) notation, E_k is the ratio between the maximum chl-specific photosynthetic rate and the maximum light utilization coefficient, $E_k = P_m^*/\alpha^*$ (the * superscript indicates an instantaneous value). Based on the recent work by Behrenfeld et al. (2004), we assume that $P_m^* = f_P^T\, f_P^f\, f_P^s\, r_P^0 P_c/P_l$ and $\alpha^* = f_P^T\, f_P^f\, f_P^s \alpha_{chl}^0$, where α_{chl}^0 is the maximum slope of the production-irradiance curve at optimal conditions. This parameterization implies that variations due to environmental factors other than light acclimation in the parameters of the production-irradiance curve are correlated (i.e. E_k-independent, according to Behrenfeld et al., 2004). The non-dimensional regulating factor for light (17) takes thus the form:

$$f_P^E = 1 - \exp\left(-\frac{\alpha_{chl}^0 E_{PAR} P_l}{r_P^0 P_c}\right). \tag{18}$$

Temperature dependence f_P^T in (16) takes the form written in eq. (7), silicate regulation is parameterized as an external limiting factor with a Michaelis-Menten form $f^s = \frac{N^{(5)}}{N^{(5)}+h_s}$ ($f^s = 1$ for the groups other than diatoms), and iron limitation f^f is described below in Sec. 5.1.3. All the nutrient regulating factors f apart from temperature have non-dimensional values between 0 and 1.

The activity exudation rate in (10) is written as:

$$\left.\frac{\partial P_c}{\partial t}\right|_{R_c^{(1)}}^{exu} = \left[\beta_P + (1-\beta_P)\left(1 - f_P^{n,p}\right)\right] \left.\frac{\partial P_c}{\partial t}\right|_{O^{(3)}}^{gpp} \tag{19}$$

and is composed of a constant fraction of carbon uptake (β_P) and a nutrient-related complementary fraction, which is controlled by the internal nutrient ratios according to the following Liebig-like regulating factor (always constrained between 0 and 1):

$$f_P^{n,p} = \min\left(\frac{P_n/P_c - n_P^{\min}}{n_P^{opt} - n_P^{\min}}, \frac{P_p/P_c - p_P^{\min}}{p_P^{opt} - p_P^{\min}}\right) \tag{20}$$

The optimal (Redfield-like) and minimum nutrient quota are indicated as n_P^{opt}, $n_P^{\min}$ for nitrogen and p_P^{opt}, $p_P^{\min}$ for phosphorus, respectively. Respiration is written as:

$$\left.\frac{\partial P_c}{\partial t}\right|_{O^{(3)}}^{rsp} = b_P P_c + \gamma_P \left\{ \left.\frac{\partial P_c}{\partial t}\right|_{O^{(3)}}^{gpp} - \left.\frac{\partial P_c}{\partial t}\right|_{R_c^{(1)}}^{exu} \right\} \tag{21}$$

and is composed of a metabolic part (with constant specific rate b_P) and a fraction γ_P of the assimilated production. The lysis products are a function of the intracellular nutrient-stress, and are partitioned into particulate and dissolved detritus according to a variable fraction $\varepsilon_P^{n,p} = \min\left(1, \frac{p_P^{\min}}{P_p/P_c}, \frac{n_P^{\min}}{P_n/P_c}\right)$, which forces the release to be particulate when nutrients are at the minum value. The total carbon release through lysis is written as:

$$\sum_{j=1,6} \left.\frac{\partial P_c}{\partial t}\right|_{R_c^{(j)}}^{lys} = \frac{1}{f_P^{p,n} + h_P^{p,n}} d_P^0 P_c \tag{22}$$

The uptake of nutrients is regulated by a Droop kinetic as detailed in Baretta-Bekker et al. (1997) and Vichi (2002):

$$\sum_{i=3,4} \left.\frac{\partial P_n}{\partial t}\right|_{N^{(i)}}^{upt} = \min\left(\left(a_P^3 N^{(3)} + a_p^4 N^{(4)}\right) P_c,\, n_P^{opt} G_P + f_P^T r_P^0 \left(n_P^{\max} - \frac{P_n}{P_c}\right) P_c \right) \tag{23}$$

$$\left.\frac{\partial P_p}{\partial t}\right|_{N^{(1)}}^{upt} = \min\left(a_P^1 N^{(1)} P_c,\, p_P^{opt} G_P + f_P^T r_P^0 \left(p_P^{\max} - \frac{P_p}{P_c}\right) P_c \right) \tag{24}$$

where G_P is the net production, the algebraic sum of the first 4 terms on the right hand side of eq. (10) and the a constants are the membrane affinity for nitrate, ammonium and phosphate (see Appendix). If the nitrogen uptake rate (23) is positive, then the partitioning between $N^{(3)}$and $N^{(4)}$uptake is done using the ratios $\frac{a_P^3 N^{(3)}}{a_P^3 N^{(3)} + a_P^4 N^{(4)}}$and $\frac{a_P^4 N^{(4)}}{a_P^3 N^{(3)} + a_P^4 N^{(4)}}$, respectively. If it is negative, as in the case of dark respiration, the whole flux is directed to the ammonium pool $N^{(4)}$.

The lysis process affects phytoplankton nutrient content proportionally to the total carbon loss in (22) with the exception that the particulate fraction has always the minimum allowed N:C or P:C ratios. For phosphorus in phytoplankton, the equations are:

$$\left.\frac{\partial P_p}{\partial t}\right|_{R_p^{(6)}}^{lys} = p_P^{\min} \left.\frac{\partial P_c}{\partial t}\right|_{R_c^{(6)}}^{lys} \tag{25}$$

$$\left.\frac{\partial P_p}{\partial t}\right|_{R_p^{(1)}}^{lys} = \left(\frac{P_p}{P_c} - p_P^{\min}\right) \left.\frac{\partial P_p}{\partial t}\right|_{R_c^{(1)}, R_c^{(6)}}^{lys} \tag{26}$$

The equations for N can be derived likewise.

For the silicate dynamics (13) there is no storage in the cytoplasm (but only in the exostructure) and silicate is released only in particulate form proportionally to the carbon lysis:

$$\left.\frac{\partial P_s^{(1)}}{\partial t}\right|_{N^{(5)}}^{upt} = s_{P^{(1)}}^{\max} G_{P^{(1)}} \tag{27}$$

$$\left.\frac{\partial P_s^{(1)}}{\partial t}\right|_{R_s^{(6)}}^{lys} = \frac{P_s^{(1)}}{P_c^{(1)}} \left.\frac{\partial P_c^{(1)}}{\partial t}\right|_{R_c^{(6)}}^{lys} \tag{28}$$

5.1.2 Chlorophyll dynamics

The chl equation written in (14) is composed of two terms. The first one is chlorophyll synthesis, which is mostly derived from Geider et al. (1996, 1997) with some adaptations to the ERSEM features, and the second one represent the losses due to grazing.

Net chl synthesis is a complicated function of acclimation to light conditions, nutrient availability (mainly N and Fe) and turnover rate. The former process is taken into account by Geider's parameterization, while the latter is generally parameterized with different formulations,for instance by assuming a dependence on gross carbon uptake (Geider et al., 1997; Blackford et al., 2004) and/or on nitrogen assimilation (Geider et al., 1998; Flynn et al., 2001). To integrate these processes into the ERSEM formulation, it is assumed that nutrient-stressed cells that release substantial amount of DOC tend to regulate their internal chl:C ratio as well, therefore we write net synthesis as a direct function of net carbon assimilation:

$$\left.\frac{\partial P_l}{\partial t}\right|^{syn} = \rho_{chl} \left(\left.\frac{\partial P_c}{\partial t}\right|_{O^{(3)}}^{gpp} - \left.\frac{\partial P_c}{\partial t}\right|_{R_c^{(i)}}^{exu} - \left.\frac{\partial P_c}{\partial t}\right|_{O^{(3)}}^{rsp} - \left.\frac{\partial P_c}{\partial t}\right|_{R_c^{(i)}}^{lys} \right). \tag{29}$$

This rate is primarily controlled by the dynamical chl:C ratio ρ_{chl} proposed by Geider et al. (1997) which regulates the amount of chl in the cell according to a non-dimensional ratio between the realized photosynthetic rate in (16) and the maximum potential photosynthesis:

$$\rho_{chl} = \theta_{chl}^0 \frac{\left.\frac{\partial P_c}{\partial t}\right|_{O^{(3)}}^{gpp}}{\alpha^* E_{PAR} P_l} \tag{30}$$

and multiplying by a maximum chl:C ratio θ_{chl}^0 different for each phytoplankton functional group (see Appendix).

According to the notation shown in the previous section, the original Geider's formulation is rewritten after some algebra as:

$$\rho_{chl} = \theta^0_{chl} \frac{f^E_P r^0_P P_c}{\alpha^0_{chl} E_{PAR} P_l} \tag{31}$$

The ratio is down-regulated when the rate of light absorption (governed by the quantum efficiency and the amount of pigments themselves) exceeds the rate of utilization of photons for carbon fixation, as explained in detail in Geider et al. (1996).

The losses of chl are not explicitly taken into account in the model because we have currently not implemented a chl component in detritus and dissolved organic matter. The same consideration applies to the ingested chl fraction in zooplankton. All these terms are presently collected into a generic sink term that is used for mass conservation purposes, but can be easily split into its major components once it is seen necessary to follow the degradation products of chl (e.g. phaeopigments) in a global context.

5.1.3 Iron dynamics

It is currently recognized that iron in the ocean is a crucial regulator of the productive phase of marine phytoplankton. In the past 15 years, the "iron hypothesis" (Martin et al., 1991) has been verified by means of open ocean iron fertilization experiments (Martin et al., 1994; Boyd et al., 2000) and experimental studies of iron chemistry and bioavailability (Coale et al., 1996; Sunda and Huntsman, 1997; Price, 2005). It is however still unclear how much of the actual carbon export depends on the iron availability and which mechanisms control the supply of iron to the euphotic zones from the major geochemical sources (Johnson et al., 1997; Fung et al., 2000). Iron is included in the model (Fig. 3 and Tab. 1) as an inorganic CFF representing dissolved form $N^{(7)}$, as a living organic CFF of phytoplankton and a non-living organic CFF for particulate detritus (units are μmol m^{-3}). Iron in the water is thought to be almost entirely bound in complex molecules by means of organic ligands (Johnson et al., 1997) and the concentration of dissolved inorganic iron [Fe'] has a very small solubility limit (~0.75 nM at 20°C and pH = 8.1-8.2) over which hydroxides are formed and adsorbed onto sinking particles. Recent studies (Kraemer, 2004) have shown that bacteria produce molecules called siderophores to which dissolved Fe(III) binds. The photochemical reaction helps to transform the iron complexes into a Fe(II)-based form that enables other marine organisms to acquire it. Since these processes are still being investigated, the effect of iron ligands and bacterial complexation is currently neglected. State variable $N^{(7)}$ thus represents all the bioavailable iron [Fe'] but since iron is considered an internal component of all the functional groups, the model can be easily expanded to introduce new important concepts.

The equation (15) for iron in phytoplankton P_f contains a term for the uptake of [Fe'], a loss term related to turnover/cell lysis and a predation term. In most models, it is assumed that cellular Fe is in constant proportion with C. However, by linearly interpolating culture data under different [Fe'], Sunda and Huntsman (1997) found that the Fe:C ratio needed for cell maintenance at zero growth rate is close to 3 μmol Fe:mol C (~330,000 mol C:mol Fe) and phytoplankton linearly increase the intracellular Fe:C ratio as a function of external [Fe'] for saturating light conditions (Sunda and Huntsman, 1995, see their Fig. 3). Therefore a value of 2-3 represents the minimum internal ratio for cell survival, but it is not simple to find one single constant value representative of the optimal cellular requirement (Sunda, 1997). Ho et al. (2003) derived an optimal value of 60 for the average stoichiometry of the soft tissues of some marine phytoplankton species cultivated in non-limiting media ($(C_{124})_{1000}Fe_{7.5}$). Data from Sunda and Huntsman (1995) show that saturation of growth rate is achieved when the intracellular ratio is above 20, depending on light conditions. The prescribed value of the optimal ratio is $\phi_P^{opt} = 6$ μmol Fe:mol C, closer to the constant ratios assumed by other authors in their models (Leonard et al., 1999; Aumont et al., 2003). Similarly to N and P content, intracellular Fe:C quota are allowed to vary between a maximum and a minimum thresholds (ϕ_P^{max} and ϕ_P^{min}, see values in Appendix), and the realized quotum is used to derive a non-dimensional regulating factor as in eq. (20):

$$f_P^f = \frac{P_f/P_c - \phi_P^{min}}{\phi_P^{opt} - \phi_P^{min}} \tag{32}$$

The allowed minimum ratio ϕ_P^{min} represents the evolutive adaptation of each functional group at the prevailing iron concentrations, and the optimal value ϕ_P^{opt} indicates the cellular requirement for optimal growth. Minimum values are smaller for picophytoplankton and higher for diatoms, according to observations and surface:volume ratio considerations (Strzepek and Harrison, 2004; Timmermans et al., 2004, 2005). This regulating factor modulates the actual photosynthetic rate in eq. (16) since there is a clear decrease in the activity of PSUs due to insufficient cellular Fe (Sunda and Huntsman, 1997).

The regulating factor inhibits carbon fixation, but iron can still be uptaken in the cell, progressively increasing the internal quotum. Iron uptake from dissolved pools is computed according to Droop kinetics by taking the minimum of two rates, a linear function of the ambient concentration simulating the membrane through-flow at low external Fe concentration, and the balancing flux according to the carbon assimilation as in the case of N and P macronutrients (23-24):

$$\left.\frac{\partial P_f}{\partial t}\right|_{N^{(7)}}^{upt} = \min\left(a_P^7 N^{(7)} P_c,\ \phi_P^{opt} G_P + f_P^T r_P^0 \left(\phi_P^{max} - \frac{P_f}{P_c}\right) P_c\right) \tag{33}$$

Direct iron excretion from phytoplankton is still an unknown biochemical pathway, therefore we assume that the only physiological iron loss from phytoplankton is

linked to cell disruption, computed according to carbon lysis and assuming that particulate material has the minimum structural Fe:C ratio:

$$\left.\frac{\partial P_f}{\partial t}\right|_{R_f^{(6)}}^{lys} = \phi_P^{min} \left.\frac{\partial P_c}{\partial t}\right|_{R_c^{(6)}}^{lys}. \tag{34}$$

5.2 Zooplankton

The zooplankton LFGs in the model are: omnivorous mesozooplankton $Z_i^{(4)}$, comprising any permanent member of the zooplankton community which is between 200 μm and 3 to 4 cm long as an adult; microzooplankton., state variable $Z_i^{(5)}$, representing the biomass concentration of microzooplankton with a ESD in the range 20- 200 μm, and heterotrophic nanoflagellates, state variable $Z_i^{(6)}$, which are protozoa with dimensions between 2 and 20 μm, mainly grazing upon picophytoplankton and bacteria. These latter groups also embrace many mesozooplankton species that are traditionally considered part of the microzooplankton when in juveniles stages (Broekhuizen et al., 1995).

Zooplankton parameterization is derived from Baretta-Bekker et al. (1995) and Broekhuizen et al. (1995). Both micro- and mesozooplankton groups also indulge in "cannibalism", preying on other members of their own functional group. The zooplankton equations parameterize the processes of growth due to ingestion and the loss terms due to excretion/egestion, mortality, respiration and predation due to other zooplankters. Each zooplankton LFG comprises 3 CFFs for C, N and P content:

$$\left.\frac{\partial Z_c}{\partial t}\right|_{bio} = \sum_{X=P,Z} \left.\frac{\partial Z_c}{\partial t}\right|_{X_c}^{prd} - \sum_{j=1,6} \left.\frac{\partial Z_c}{\partial t}\right|_{R_c^{(j)}}^{rel} - \left.\frac{\partial Z_c}{\partial t}\right|_{O^{(3)}}^{rsp} - \sum_{k=4,5,6} \left.\frac{\partial Z_c}{\partial t}\right|_{Z_c^{(k)}}^{prd} \tag{35}$$

$$\left.\frac{\partial Z_n}{\partial t}\right|_{bio} = \frac{F_n}{F_c} \sum_{X=P,Z} \left.\frac{\partial Z_c}{\partial t}\right|_{X_c}^{prd} - \sum_{j=1,6} \left.\frac{\partial Z_n}{\partial t}\right|_{R_n^{(j)}}^{rel} - \left.\frac{\partial Z_n}{\partial t}\right|_{N^{(4)}}^{rel} - \frac{Z_n}{Z_c} \sum_{k=4,5,6} \left.\frac{\partial Z_c}{\partial t}\right|_{Z_c^{(k)}}^{prd} \tag{36}$$

$$\left.\frac{\partial Z_p}{\partial t}\right|_{bio} = \frac{F_p}{F_c} \sum_{X=P,Z} \left.\frac{\partial Z_c}{\partial t}\right|_{X_c}^{prd} - \sum_{j=1,6} \left.\frac{\partial Z_p}{\partial t}\right|_{R_p^{(j)}}^{rel} - \left.\frac{\partial Z_p}{\partial t}\right|_{N^{(1)}}^{rel} - \frac{Z_p}{Z_c} \sum_{k=4,5,6} \left.\frac{\partial Z_c}{\partial t}\right|_{Z_c^{(k)}}^{prd} \tag{37}$$

We currently do not consider Si, Fe and chl as living CFFs for zooplankton. This is a reasonable approximation for Si, because biogenic silica in the form of frustiles is directly egested by zooplankters. Chl is a negligible part of C and N in the total biomass of preys, but the absence of internal Fe dynamics implies that the iron content of ingested food does not affect zooplankton net growth as instead occurs for N and P. In addition, we neglect the explicit recycling pathways of Fe through zooplankton activity (Schmidt et al., 1999) which are instead parameterized implicitly as shown below in eq. (69).

The total amount of food available to zooplankton is computed considering the set of possible preys $X_i \in \left\{ P_i^{(j)}, B_i, Z_i^{(j)} \right\}$ as the vector $F_i = \sum_X \delta_{Z,X} e_{Z,X} X_i$, where $\delta_{Z,X}$ is the availability of predator Z for prey X_i and $e_{Z,X}$ is the capture efficiency. The product of the latter terms gives the total preference. There are many definitions of preferences in the literature, and we have used concepts from Gentleman et al. (2003) and Gibson et al. (2005) to combine the parameterizations described in Baretta-Bekker et al. (1995) for microzooplankton and in Broekhuizen et al. (1995) for mesozooplankton. Availability represents the quality of the prey and is assumed to be mostly dependent on the prey nominal dimensions (see Appendix). Capture efficiency (or relative preference) is also a non-dimensional factor which is set to 1 for mesozooplankton and is density-dependent in microzooplankton, $e_{Z,X} = \frac{X_c}{X_c + \mu_Z}$, according to the threshold half-saturation density μ_Z ($\mu_Z = 0$ for mesozooplankton).

The first term on the right hand side of eq. (35) is the total carbon ingestion, which corresponds to the sum of all the predation loss terms in the carbon equations of the other functional groups preyed by zooplankton. Applying the inter-functional group conversion defined in (6), the rate term for each predation processes is parameterized with a Type 2 formulation (Gentleman et al., 2003),

$$\left.\frac{\partial Z_c}{\partial t}\right|_{X_c}^{prd} = -\left.\frac{\partial X_c}{\partial t}\right|_{Z_c}^{prd} = f_Z^T \, r_Z^0 \frac{\delta_{Z,X} e_{Z,X} X_c}{F_c} \frac{F_c}{F_c + h_Z^F} Z_c \tag{38}$$

which is traditionally rewritten in terms of the specific search volume in the case of mesozooplankton ($h_Z^F = \frac{r_{0Z}}{v_Z}$), because this parameter is generally available in the literature. For brevity, in the zooplankton equations we will use the following notation to indicate the total ingestion rate in units of the BBCs:

$$\Im_i = \sum_X \left.\frac{\partial Z_i}{\partial t}\right|_{X_i}^{prd} \quad j = c, n, p. \tag{39}$$

Metabolic rates in zooplankton are assumed to be closely coupled to growth, therefore total ingested carbon is used part for net production, part for respiration and the remainder is egested/excreted. The parameters that can be measured in laboratory experiments are net growth efficiency η_Z (the ratio between net secondary production and the sum of net production and activity respiration) and the egested portion of ingested material β_Z (also taking into account sloppy feeding). From the point of view of stoichiometric ecology, we notice here that the ingestion rate in eq. (39) is not directly affected by prey quality in our present formulation (Mitra and Flynn, 2005). Nevertheless, the definition of constant optimal nutrient quota in zooplankton (Baretta-Bekker et al., 1997), equivalent to the Threshold Elemental Ratios of Andersen et al. (2004, TER), implies that the ingestion of low-quality (i.e. nutrient-poor) food lead to the disposal of the ingested carbon in excess, thus effectively limiting biomass growth.

On the other hand, an excess of nutrients, as for instance due to the ingestion of phytoplankton under "luxury uptake" conditions, leads to an increase of the nutrient remineralization rates as shown below in eqs. (45-46). The release of extra C is parameterized as an increase of the egestion rates of organic carbon compounds or, in alternative, by increasing the respiration rates. Both processes are well documented in freshwater zooplankton (Frost et al., 2004; Anderson, 2005) and we have decided to parameterize the increase of excretion rates. The two pathways are equivalent from the point of view of internal element regulation in zooplankton, but the consequences of one choice or another on the biogeochemical cycling of carbon are still to be investigated both experimentally and in model studies.

The carbon loss term in (35) thus represents the sum of the activity excretion/egestion (higher for mesozooplankton because of sloppy feeding), the mortality rates and the nutrient-limited excretion of organic carbon:

$$\sum_{j=1,6} \frac{\partial Z_c}{\partial t}\bigg|_{R_c^{(j)}}^{rel} = \beta_Z \Im_c + d_{0_Z} f_Z^T Z_c + d_Z^{dns} Z_c^{\gamma_Z} + Q_Z^c \tag{40}$$

The released fraction is further divided into particulate (faecal pellets) and dissolved organic forms using a constant percentage ε_Z^c (mesozooplankton is assumed to have no dissolved products). Mortality is parameterized as senescence with a first-order constant rate d_{0_Z} and a grazing closure by higher trophic levels not resolved in the model, which is a power function of density valid only for mesozooplankton ($d_Z^{dns} = 0$ for microzooplankton).

The balancing flow of C Q_Z^c is computed from the actual elemental ratios of ingested material:

$$\Gamma_Z^i = \frac{(1-\beta_Z)\Im_c}{\eta_Z \Im_c}, \quad i = n, p \tag{41}$$

which are cross-compared with the optimal (constant) TERs, n_Z^{opt} and p_Z^{opt}. If nitrogen is limiting $\left(\Gamma_Z^n < n_Z^{opt}\right)$, and/or phosphorus is limiting $\left(\Gamma_Z^p < p_Z^{opt}\right)$, then

$$Q_Z^c = \eta_Z \Im_c - \frac{(1-\beta_Z)}{n_Z^{opt}} \Im_n - \frac{(1-\beta_Z)}{p_Z^{opt}} \Im_p, \tag{42}$$

otherways $Q_Z^c = 0$.

Taking into account the activity excretion in eq. (40) and after some algebra, the total respiration rate can be written as:

$$\frac{\partial Z_c}{\partial t}\bigg|_{O^{(3)}}^{rsp} = (1-\beta_Z)(1-\eta_Z)\Im_c + b_Z f_Z^T Z_c \tag{43}$$

where the constant body-respiration rate b_Z is also considered.

The nutrient dynamics for zooplankton given in eqs. (36) and (37) are mainly derived from carbon dynamics taking into account the nutrient content of the total

food uptake. The excretion/egestion rate of organic nutrients is obtained from eq. (40) as:

$$\sum_{j=1,6} \left.\frac{\partial Z_i}{\partial t}\right|_{R_i^{(j)}}^{rel} = \frac{Z_i}{Z_c}\left(\beta_Z \Im_c + d_{0Z} f_Z^T Z_c + d_Z^{dns} Z_c^{\gamma_Z}\right), \quad i = n, p \tag{44}$$

and is subsiquently partitioned between particulate and dissolved according to the non-dimensional fraction ε_Z^i which parameterizes the different distribution of nutrients between structural parts and cytoplasm (see values in Appendix).

The third terms on the right hand side of eq. (36) and (37) parameterize the zooplankton excretion of inorganic nutrients, which occur only when the internal nutrient quota exceed the optimal quota for P and N, p_Z^{opt} and n_Z^{opt}, respectively. The following formulations allow organisms to have temporary imbalance in their nutrient content:

$$\left.\frac{\partial Z_p}{\partial t}\right|_{N^{(1)}}^{rel} = \nu_Z^p \max\left(0, \frac{Z_p}{Z_c} - p_Z^{opt}\right) Z_p \tag{45}$$

$$\left.\frac{\partial Z_n}{\partial t}\right|_{N^{(4)}}^{rel} = \nu_Z^n \max\left(0, \frac{Z_n}{Z_c} - n_Z^{opt}\right) Z_n \tag{46}$$

and the time scales of excretion are controlled by the specific constant rates ν_Z^p and ν_Z^n (see Appendix). The excretion is in the form of phosphate and urea, but the latter in the model is assumed to be as labile as the ammonium, therefore the rate is directed to the $N^{(4)}$ pool.

5.3 Bacterioplankton

The equations for bacterioplankton are written in a similar manner to the ones for *P* and *Z* living functional groups. The bacteria LFG comprises 3 CFFs for the C, N and P content, with 3 dynamical equations that have been recently formulated by (Vichi et al., 2003b) and extended to include denitrification and anaerobic processes in Vichi et al. (2004). Bacteria are heterotrophs and their production rates depend directly from the availability of organic substrate. The original ERSEM papers did not include any prognostic variable for dissolved organic matter (DOM), which was assumed to be directly available to bacteria within the same day of production. The CFFs representing organic matter are divided into a particulate and a dissolved fraction written in terms of C, N, P and Si content (the latter for particulate only, cfr. Tab. 1 and Sec. 5.4.3). As shown in the previous sections, the nutrient content of freshly-produced DOM and detritus is set by the other LFGs according to their internal nutrient quota.

Bacterial physiological processes are uptake of organic substrate (*upt*) and uptake or remineralization of inorganic nutrients (*upt,rel*), but are not assumed to release organic matter (e.g. capsular material), therefore their loss terms are limited to respiration and predation:

$$\left.\frac{\partial B_c}{\partial t}\right|_{bio} = \sum_{j=1,6} \left.\frac{\partial B_c}{\partial t}\right|_{R_c^{(j)}}^{upt} - \left.\frac{\partial B_c}{\partial t}\right|_{O^{(3)}}^{rsp} - \sum_{k=5,6} \left.\frac{\partial B_c}{\partial t}\right|_{Z_c^{(k)}}^{prd} \tag{47}$$

$$\left.\frac{\partial B_n}{\partial t}\right|_{bio} = \sum_{j=1,6} \frac{R_n^{(j)}}{R_c^{(j)}} \left.\frac{\partial B_c}{\partial t}\right|_{R_c^{(j)}}^{upt} + f_B^n \left.\frac{\partial B_n}{\partial t}\right|_{N^{(4)}}^{upt,rel} - \frac{B_n}{B_c} \sum_{k=5,6} \left.\frac{\partial B_c}{\partial t}\right|_{Z_c^{(k)}}^{prd} \tag{48}$$

$$\left.\frac{\partial B_p}{\partial t}\right|_{bio} = \sum_{j=1,6} \frac{R_p^{(j)}}{R_c^{(j)}} \left.\frac{\partial B_c}{\partial t}\right|_{R_c^{(j)}}^{upt} + f_B^p \left.\frac{\partial B_p}{\partial t}\right|_{N^{(1)}}^{upt,rel} - \frac{B_p}{B_c} \sum_{k=5,6} \left.\frac{\partial B_c}{\partial t}\right|_{Z_c^{(k)}}^{prd} \tag{49}$$

The realized total carbon uptake rate of organic substrate in (47) is regulated by environmental factors and substrate availability in a Liebig-like formulation:

$$\sum_{j=1,6} \left.\frac{\partial B_c}{\partial t}\right|_{R_c^{(j)}}^{upt} = \min\left(f_B^{n,p} Q_{10}^{\frac{T-10}{10}} r_B^0 B_c, \nu_{R^{(6)}} f_{R^{(6)}}^{n,p} R_c^{(6)} + \nu_{R^{(1)}} f_{R^{(1)}}^{n,p} R_c^{(1)} \right), \tag{50}$$

where the first term between brackets is the bacterial growth at a given temperature, r_B^0 is the maximum potential growth rate (see value in Appendix) and $f_B^{n,p}$ is the non-dimensional regulating factor parameterizing the internal nutritional status of bacteria:

$$f_B^{n,p} = \min\left(\frac{B_p/B_c}{p^{opt}}, \frac{B_n/B_c}{n^{opt}} \right). \tag{51}$$

The second term is the availability of substrate, parameterized by a regulating factor linked to the "quality" of organic matter, i.e. the nutrient content, which can be used as a proxy for the degree of lability (Ogawa and Tanoue, 2003):

$$f_{R^{(j)}}^{n,p} = \min\left(\frac{R_p^{(j)}/R_c^{(j)}}{p^{opt}}, \frac{R_p^{(j)}/R_c^{(j)}}{n^{opt}} \right) \; j = 1,6 \tag{52}$$

The constant parameters $\nu_{R^{(j)}}$ in eq. (50) mark the nominal degree of lability of detritus and DOM, which is further modulated by their nutrient content.

Bacterial respiration is a measure of remineralization activity, and is written to take into account chemotrophic processes such as denitrification and sulphate reduction. Respiration comprises basal and activity rates as:

$$\left.\frac{\partial B_c}{\partial t}\right|_{O^{(3)}}^{rsp} = b_B f_B^T B_c + \left[1 - \eta_B + \eta_B^o \left(1 - f_B^o\right)\right] \sum_{j=1,6} \left.\frac{\partial B_c}{\partial t}\right|_{R_c^{(j)}}^{upt} \tag{53}$$

The potential bacterial growth efficiency η_B controls the quota of carbon that is respired for metabolic processes and this portion increases of a quantity η_B^o as a steep sigmoidal function of the ambient oxygen concentration

$$f_B^o = \frac{\left(O^{(2)}\right)^3}{\left(O^{(2)}\right)^3 + \left(h_B^o\right)^3} \tag{54}$$

to parameterize the lower efficiency of anaerobic metabolism (see Appendix for a list of parameter values and description). Eqs. (53) and (54) are used below to derive the bacterial oxygen demand and/or the demand of other oxidized inorganic species such as nitrate (Sec. 5.4.2) and sulphate.

Depending on their internal nutrient:carbon ratios, bacteria can behave as remineralizers or as competitors with phytoplankton, taking up inorganic nutrients directly from the water. The optimal nutrient quota for P and N p_B^{opt} and n_B^{opt} regulate the intensity of this process:

$$\left.\frac{\partial B_p}{\partial t}\right|_{N^{(1)}}^{upt,rel} = f_B^p \nu_B^p \left(\frac{B_p}{B_c} - p_B^{opt}\right) B_c \tag{55}$$

$$\left.\frac{\partial B_n}{\partial t}\right|_{N^{(4)}}^{upt,rel} = f_B^n \nu_B^n \left(\frac{B_n}{B_c} - n_B^{opt}\right) B_c \tag{56}$$

and the sign is controlled by the non-dimensional factors f_B^p and f_B^n and by the specific constant rates ν_B^p and ν_B^n. In the case of phosphorus, for instance, if $\frac{B_p}{B_c} - p_B^{opt} > 0$ (excretion of nutrients) the non-dimensional parameter $f_B^p = -1$, and if $\frac{B_p}{B_c} - p_B^{opt} < 0$ there is direct uptake from the water as a function of the nutrient concentration in a Michaelis-Menten form, $f_B^p = \frac{N^{(1)}}{N^{(1)} + h_B^p}$.

5.4 Chemical functional families

5.4.1 Oxygen, carbon dioxide and anoxic processes

The dynamics of dissolved oxygen and carbon dioxide are important closures of global biogeochemical cycles. We do not describe here the exchange of gases at the air sea interface which is assumed to be a purely physical process and has been thoroughly investigated elsewhere, especially for CO_2 (Olsen et al., 2005).

Anaerobic processes and denitrification dynamics are a consequence of oxygen dynamics and are described here for completeness, although they are of limited impact in the well-oxygenated euphotic zones of the open ocean. Nevertheless, these processes are important for the sulfur cycle and for the fate of exported carbon in

the meso- and bathypelagic layers of the ocean where bacteria are the major drivers of these processes. To account for hypoxic and anoxic remineralization in the water, the original ERSEM parameterization of anaerobic processes in the sediments proposed by Ruardij and Van Raaphorst (1995) was extended to the pelagic system by Vichi et al. (2004). The state variable "reduction equivalents" $N^{(6)}$ (Table 1 and Fig. 3) is an inorganic CFF state variable containing all the reduced chemical species and assumed to be chemically equivalent to the sulphide ion HS^-. The basic constituent is indicated with the letter R because this variable account for all the reduced biochemical products, although it should be mostly regarded as sulphur S. Reduction equivalents are produced as a result of bacterial anoxic respiration and are partly used for the parameterization of denitrification processes and partly for direct sulphide production. We refer to Vichi et al. (2004) for major details on the parameterization and for an application to the Baltic Sea.

The pelagic net production of oxygen is derived from the sum of gross primary production and community respiration rates from phytoplankton, zooplankton and bacteria, also subtracting the losses due to pelagic chemical reactions:

$$\left.\frac{\partial O^{(2)}}{\partial t}\right|_{bio} = \Omega_c^o \sum_{j=1}^{3} \left(\left.\frac{\partial P_c^{(j)}}{\partial t}\right|_{O^{(3)}}^{gpp} - \left.\frac{\partial P_c^{(j)}}{\partial t}\right|_{O^{(3)}}^{rsp} \right) - \Omega_c^o f_B^o \left.\frac{\partial B_c}{\partial t}\right|_{O^{(3)}}^{rsp} + \\ -\Omega_c^o \sum_{j=4}^{6} \left.\frac{\partial Z_c^{(j)}}{\partial t}\right|_{O^{(3)}}^{rsp} - \Omega_n^o \left.\frac{\partial N^{(4)}}{\partial t}\right|_{N^{(3)}}^{nit} - \frac{1}{\Omega_o^r} \left.\frac{\partial N^{(6)}}{\partial t}\right|_{sink_r}^{reox} \tag{57}$$

All the rates are converted into oxygen units by means of stoichiometric coefficients given (see Appendix). Since bacteria are active both under aerobic and anaerobic conditions the bacterial oxygen demand (53) is partitioned into oxygen consumption and reduction equivalent production by using the oxygen regulating factor f_B^o in (54). The nitrification rate is a source term of the nitrate equation (64), and a sink term for ammonium (65) and oxygen (57). Nitrification is not explicitly resolved but parameterized with a simple first-order dependence on ammonium and oxygen concentrations:

$$\left.\frac{\partial N^{(4)}}{\partial t}\right|_{N^{(3)}}^{nit} = \Lambda_{N^{(4)}}^{nit} f_{N^{(4)}}^T \frac{O^{(2)}}{O^{(2)} + h_{N^{(4)}}^o} N^{(4)} \tag{58}$$

where Λ_{N4}^{nit} is the constant specific nitrification rate and f^T a temperature regulating factor with the Q10 formulation shown in (7).

The formation of reduction equivalents is parameterized converting the biological oxygen demand of bacteria (under low oxygen conditions) into sulphide ions by using the stoichiometric coefficient Ω_o^r (see Appendix) as:

$$\left.\frac{\partial N^{(6)}}{\partial t}\right|_{bio} = \Omega_o^r \Omega_c^o \left(1 - f_{B1}^o\right) \left.\frac{\partial B_c}{\partial t}\right|_{O^{(3)}}^{rsp} - \Omega_o^r \widetilde{\Omega}_n^o \left.\frac{\partial N^{(3)}}{\partial t}\right|_{sink_n}^{denit} - \left.\frac{\partial N^{(6)}}{\partial t}\right|_{sink_r}^{reox} \tag{59}$$

The utilization of nitrate as an electron acceptor in microbial metabolic reactions is parameterized in an indirect way. Firstly, when the oxygen level falls below the threshold level and $f^o_{B1} < 1$ (eq. (54)), the metabolic formation of reduction equivalents begins according to the carbon mineralization rate (53). The denitrification reaction is favored with respect to the pure anaerobic sulpho-reduction, therefore a portion of this oxygen demand is redirected towards the denitrification process. In order to achieve this net effect, the changes in the redox conditions enhance the denitrification flux in the following way:

$$\left.\frac{\partial N^{(3)}}{\partial t}\right|^{denit} = \Lambda^{denit}_{N^{(3)}} \left[\frac{1}{\mathcal{M}^*_o}\Omega^o_c \left(1 - f^o_B\right) \left.\frac{\partial B_c}{\partial t}\right|^{rsp}_{O^{(3)}}\right] N^{(3)}. \tag{60}$$

where $\Lambda^{denit}_{N^{(3)}}$ is the specific denitrification rate at a reference anoxic mineralization $\mathcal{M}^*_o$ (see Appendix for a list of parameter values). If nitrate is still present in the water, the bacterial rate of production of reduction equivalents $N^{(6)}$ is converted to nitrate consumption, mimicking the bacteria-mediated denitrification reactions. Note that this chemical rate does not lead to a direct production of gaseous N_2 in the water, because this variable is not currently defined in the model.

Furthermore, as long as there is some oxygen left, reduction equivalents are also quickly reoxidized at the following rate:

$$\left.\frac{\partial N^{(6)}}{\partial t}\right|^{reox}_{sink_r} = \Lambda^{reox}_{N^{(6)}} f^T_{N^{(6)}} \frac{O^{(2)}}{O^{(2)} + h^o_{N^{(6)}}} N^{(6)} \tag{61}$$

where $\Lambda^{reox}_{N^{(6)}}$ is the (constant) specific daily reoxidation rate, $f^T_{N^{(6)}}$ is the temperature regulating factor given in (7) and $h^o_{N^{(6)}}$ is the half-saturation concentration (see Appendix). When oxygen and nitrate are completely depleted the last two terms in (59) become zero and the process turns to a strict anaerobic formation of sulphide ions coupled to the availability of the organic substrate.

In the current implementation of the model there is no explicit resolution of all the carbon dioxide dynamics, because CO_2 is assumed to be infinitely available in the waters and only the biological interactions are resolved. The aquatic chemistry of $CO_2$and carbonates is a further extension to the original ERSEM formulation previously published in Blackford and Burkill (2002), and the theory of its chemical reactions is well understood (Zeebe and Wolf-Gladrow, 2001). Carbonate dynamics and surface exchange processes are currently being included in PELAGOS, particularly taking into account the works done in the Ocean Carbon Model Intercomparison Project (Doney et al., 2004). The biological production and consumption of CO_2 presently considered in the model can be easily derived by collecting the first 4 terms on the right hand side of eq. (57) without considering the stoichiometric

factor Ω_c^o and taking the total bacterial respiration as

$$\left.\frac{\partial O^{(3)}}{\partial t}\right|_{bio} = \sum_{j=1}^{3}\left(\left.\frac{\partial P_c^{(j)}}{\partial t}\right|_{O^{(3)}}^{gpp} - \left.\frac{\partial P_c^{(j)}}{\partial t}\right|_{O^{(3)}}^{rsp}\right) - \left.\frac{\partial B_c}{\partial t}\right|_{O^{(3)}}^{rsp} - \sum_{k=4,5,6}\left.\frac{\partial Z_c^{(k)}}{\partial t}\right|_{O^{(3)}}^{rsp} \tag{62}$$

5.4.2 Dissolved inorganic nutrients

The pelagic cycles of dissolved inorganic nutrients are an essential component of any biogeochemical model of the marine ecosystem. Five inorganic CFFs for dissolved compounds are considered here (Fig. 3): phosphate, nitrate (nitrate + nitrite), ammonium, silicate and bioavailable iron with the following equations

$$\left.\frac{\partial N^{(1)}}{\partial t}\right|_{bio} = -\sum_{j=1}^{3}\left.\frac{\partial P_p^{(j)}}{\partial t}\right|_{N^{(1)}}^{upt} + f_B^p\left.\frac{\partial B_p}{\partial t}\right|_{N^{(1)}}^{upt,rel} + \sum_{k=4,5,6}\left.\frac{\partial Z_p^{(k)}}{\partial t}\right|_{N^{(1)}}^{rel} \tag{63}$$

$$\left.\frac{\partial N^{(3)}}{\partial t}\right|_{bio} = -\sum_{j=1}^{3}\left.\frac{\partial P_n^{(j)}}{\partial t}\right|_{N^{(3)}}^{upt} + \left.\frac{\partial N^{(3)}}{\partial t}\right|_{N^{(4)}}^{nit} - \left.\frac{\partial N^{(3)}}{\partial t}\right|_{sink_n}^{denit} \tag{64}$$

$$\left.\frac{\partial N^{(4)}}{\partial t}\right|_{bio} = -\sum_{j=1}^{3}\left.\frac{\partial P_n^{(j)}}{\partial t}\right|_{N^{(4)}}^{upt} + f_B^p\left.\frac{\partial B_n}{\partial t}\right|_{N^{(4)}}^{upt,rel} + \sum_{k=4,5,6}\left.\frac{\partial Z_n^{(k)}}{\partial t}\right|_{N^{(4)}}^{rel} - \left.\frac{\partial N^{(4)}}{\partial t}\right|_{N3}^{nit} \tag{65}$$

$$\left.\frac{\partial N^{(5)}}{\partial t}\right|_{bio} = -\left.\frac{\partial P_s^{(1)}}{\partial t}\right|_{N^{(5)}}^{upt} + \left.\frac{\partial R_s^{(6)}}{\partial t}\right|_{N^{(5)}}^{rmn} \tag{66}$$

$$\left.\frac{\partial N^{(7)}}{\partial t}\right|_{bio} = -\left.\frac{\partial P_f}{\partial t}\right|_{N^{(7)}}^{upt} + \left.\frac{\partial R_f^{(6)}}{\partial t}\right|_{N^{(7)}}^{rmn} + \left.\frac{\partial N^{(7)}}{\partial t}\right|_{sink_f}^{scv} \tag{67}$$

Most of the rates in the equations above have already been described in previous sections and will be briefly recalled here.

The pelagic cycle of phosphate $N^{(1)}$ in (63) is affected by phytoplankton uptake (23), bacterial uptake/release (55) and excretion from zooplankton groups (45).

The pelagic processes for nitrate $N^{(3)}$ shown in (64), involve phytoplankton uptake described in (11) and the nitrification and denitrification process parameterizations described in (58) and (60), respectively.

Ammonium (eq. (65)) is consumed by phytoplankton as described in (23) and remineralized (or utilized) by bacteria according to the quality of the substrate and their internal content of nitrogen according to eq. (56). Zooplankton participates to the ammonium dynamics through the excretion of urea, which is assumed to be directly available in the form of ammonium, as shown in eq. (46).

The pelagic cycle of silicate is quite simple in the model because of the many uncertainties linked to the complex dynamics of this element in the water. Silicate concentration was originally only affected by diatom uptake (27), but a simple first-order reaction parameterizing bacterial dissolution (e.g. Bidle and Azam, 2001) have been introduced accounting for the dissolution of silicate frustules as:

$$\left.\frac{\partial R_s^{(6)}}{\partial t}\right|_{N^{(5)}}^{rmn} = \Lambda_s^{rmn} f_{R^{(6)}}^T R_s^{(6)} \tag{68}$$

where Λ_s^{rmn} is the constant specific dissolution rate and $f_{R^{(6)}}^T$ is the temperature regulating factor as in eq. (7), mimicking bacterial activity enhancement at higher temperatures.

Iron is made available in dissolved form through remineralization of biogenic particles produced by phytoplankton and zooplankton. As described in Sec. 5.1.3, the biochemical pathways of the remineralization process are not completely clear and involve both syderophores and photochemical reactions. Since all these processes are primarily bacterial-mediated, it is preliminary assumed that dissolved Fe is released from detritus according to a first-order relationship as for silicate (68):

$$\left.\frac{\partial R_f^{(6)}}{\partial t}\right|_{N^{(5)}}^{rmn} = \Lambda_f^{rmn} f_{R^{(6)}}^T R_f^{(6)} \tag{69}$$

where Λ_f^{rmn} is a constant specific dissolution rate and $f_{R^{(6)}}^T$ is the temperature dependence. Both numbers are currently unknown, and therefore they need to be adjusted numerically for balancing the iron cycle in the ocean. The further inclusion of iron as an explicit component of zooplankton and bacteria may link this process to the direct excretion of organisms and bacterial regeneration activity, once the important pathways and time-scales have been properly assessed by laboratory and in situ experiments.

Dissolved inorganic iron species are scavenged onto particle surfaces owing to hydroxide precipitation. Since the concentration of iron ligands is about 0.6 nM in the deep ocean, Johnson et al. (1997) suggested that iron scavenging can be parameterized with a constant rate when the [Fe'] is above this threshold. Ligands dynamics have been further investigated by Archer and Johnson (2000); Parekh et al. (2004); Lefevre and Watson (1999), but the simplest approach proposed by Johnson et al. (1997) and Aumont et al. (2003) has been used here:

$$\left.\frac{\partial N^{(7)}}{\partial t}\right|_{sink_f}^{scv} = \Lambda_f^{scv} \min\left(0, N^{(7)} - 0.6\right) \tag{70}$$

with a given time constant $\Lambda_f^{scv} = \frac{1}{40}$ years^{-1} and with the further assumption that

scavenging results into definitive adsorption onto sinking particles and sequestration in the deeper layers.

5.4.3 Dissolved and particulate organic matter

The equations for dissolved organic matter (DOM, $R_j^{(1)}$) is linked to 3 biogeochemical basic constituents C, N and P and is thus described by 3 equations:

$$\left.\frac{\partial R_c^{(1)}}{\partial t}\right|_{bio} = \sum_{j=1}^{3} \left.\frac{\partial P_c^{(j)}}{\partial t}\right|_{R_c^{(1)}}^{exu} - \left.\frac{\partial B_c}{\partial t}\right|_{R_c^{(1)}}^{upt} + \sum_{k=5,6} \left.\frac{\partial Z_c^{(k)}}{\partial t}\right|_{R_c^{(1)}}^{rel} \tag{71}$$

$$\left.\frac{\partial R_i^{(1)}}{\partial t}\right|_{bio} = \sum_{j=1}^{3} \left.\frac{\partial P_i^{(j)}}{\partial t}\right|_{R_i^{(1)}}^{exu} - \frac{R_i^{(1)}}{R_c^{(1)}} \left.\frac{\partial B_c}{\partial t}\right|_{R_c^{(1)}}^{upt} + \sum_{k=5,6} \frac{Z_i^{(k)}}{Z_c^{(k)}} \left.\frac{\partial Z_c^{(k)}}{\partial t}\right|_{R_c^{(1)}}^{rel} \qquad i = n, p \tag{72}$$

which show that DOM is produced by phytoplankton, bacteria and microzooplankton and used as organic substrate by bacteria. The different degrees of lability of DOM are reflected in the nutrient content of $R_{(j)}^{(1)}$, which regulates bacterial uptake as shown in eq (50). Refractory organic matter is not considered in this model, because it is considered to be a background value which is constantly maintained at the global scale (Ogawa and Tanoue, 2003).

Particulate detritus is instead described by 5 equations, one for each biogeochemical basic constituent C, N, P, Si and Fe as:

$$\left.\frac{\partial R_c^{(6)}}{\partial t}\right|_{bio} = \sum_{j=1}^{3} \left.\frac{\partial P_c^{(j)}}{\partial t}\right|_{R_c^{(6)}}^{lys} - \left.\frac{\partial B_c}{\partial t}\right|_{R_c^{(6)}}^{upt} + \sum_{k=4}^{6} \left.\frac{\partial Z_c^{(k)}}{\partial t}\right|_{R_c^{(6)}}^{rel} \tag{73}$$

$$\left.\frac{\partial R_i^{(6)}}{\partial t}\right|_{bio} = \sum_{j=1}^{3} \left.\frac{\partial P_i^{(j)}}{\partial t}\right|_{R_i^{(6)}}^{lys} - \frac{R_i^{(6)}}{R_c^{(6)}} \left.\frac{\partial B_c}{\partial t}\right|_{R_c^{(6)}}^{upt} + \sum_{k=4}^{6} \frac{Z_i^{(k)}}{Z_c^{(k)}} \left.\frac{\partial Z_c^{(k)}}{\partial t}\right|_{R_c^{(6)}}^{rel} \qquad i = n, p \tag{74}$$

$$\left.\frac{\partial R_s^{(6)}}{\partial t}\right|_{bio} = \left.\frac{\partial P_s^{(1)}}{\partial t}\right|_{R_s^{(6)}}^{lys} + \frac{P_s^{(1)}}{P_c^{(1)}} \sum_{j=4}^{6} \left.\frac{\partial P_c^{(1)}}{\partial t}\right|_{Z_c^{(j)}}^{prd} - \left.\frac{\partial R_s^{(6)}}{\partial t}\right|_{N^{(5)}}^{rmn} \tag{75}$$

$$\left.\frac{\partial R_f^{(6)}}{\partial t}\right|_{bio} = \left.\frac{\partial P_f}{\partial t}\right|_{R_f^{(6)}}^{lys} + \frac{P_f}{P_c} \sum_{k=4}^{6} \left.\frac{\partial P_c}{\partial t}\right|_{Z_c^{(k)}}^{prd} - \left.\frac{\partial R_f^{(6)}}{\partial t}\right|_{N^{(7)}}^{rmn} \tag{76}$$

The carbon, nitrogen and phosphorus component of particulate detritus in (73) and (74) respectively) are produced by all the members of the planktonic community except bacteria, which are the only utilizers of this component according to (50).

The pelagic cycle of biogenic silica is instead restricted to the release of diatom frustules through mortality and other lysis processes as in (27) and via micro/mesozooplankton predation (including sloppy feeding) with the addition of the chemical dissolution shown in (68).

Particulate iron dynamics are the consequence of processes described in (34), (69) and (70). Particulate organic Fe is also derived from zooplankton egestion and mortality. It is assumed that zooplankton is never iron-limited and the iron fraction of the ingested phytoplankton is directly egested as particulate detritus.

5.5 Active sinking of biological state variables

The sinking of biogenic material is a fundamental process for the simulation of carbon sequestration in the interior of the ocean. However, the estimation of the sinking velocity w_B in eq. (4) is still parameterized in a very simplified way in the model. Only organic detritus $R_i^{(6)}$ and diatoms are allowed to sink, the former with a constant velocity that does not take into account any aggregation mechanism, and the latter is parameterized with the original ERSEM formulation (Varela et al., 1995). Diatoms reach their maximum velocity ω^{sink} as a function of the total nutrient stress $f^{nut}_{P(1)} = \min\left(f^{n,p}_{P(1)}, f^{f}_{P(1)}, f^{s}_{P(1)}\right)$ as follows:

$$w_{P(1)} = \omega^{sink} \max\left(0, l^{sink} - f^{nut}_{P(1)}\right) \tag{77}$$

where l^{sink} is the nutrient regulating factor value below which the mechanism is effective.

6 Discussion and final remarks

The representation of the biogeochemical processes of pelagic ecosystem presented here emphasizes the flows of the major biogeochemical elements from the (in)organic pelagic pools through the food web as a function of organisms' demand and trophic relationships. The basic concepts of modelling pelagic ecosystem functions or processes through the exchange of multiple biogeochemical elements incidentally originated from Redfield's consideration that different organisms interact differently with their environment, and modify the external conditions likewise. This concept is now being re-formalized in a new branch of science called "ecological stoichiometry" (Sterner and Elser, 2002) and ERSEM incorporated from the beginning a large portion of the fundamentals of this discipline. The latest paper by Elser and Hessen (2005) illustrates well this representation by defining the concept of "biosimplicity"

via stoichiometry. Complexity in marine food webs is described in terms of organism functionalities and not by species and population dynamics. Stemming from the original ERSEM approach, in this paper we wrote the practical implementation of these concepts in partial differential equations which represent the rates of change of the major Chemical Functional Families in the pelagic ecosystem.

The degree of approximation of this approach with respect to the real system is large and there will always be a strong debate on the number and kind of components that can provide a sufficient degree of connectivity with the observed functioning of marine ecosystems. We have proposed here a formal method to revisit and extend ERSEM – one of the most complex existing ecosystem models – by defining the biogeochemical components as Chemical Functional Families and Living Functional Groups. CFFs and LFGs are theoretical constructs which allow us to relate measurable properties of marine biogeochemistry to the state variables used in deterministic models. This approach is sufficiently generic that may be used to describe other existing biomass-based ecosystem model.

In a companion paper (Vichi et al., 2006, submitted) we present an application of this approach to the simulation of the major global biogeochemical processes. A global implementation implies the choice of given values for the many parameters discussed in this paper, which have to be valid in all the regions of the global ocean. We see the inclusion of physiological regulation factors and stoichiometrical considerations in the model equation as a way to simulate the adaptation mechanisms of plankton components. However, this approach increases the number of parameters, and it is therefore important that a clear definition and formalism is established to promote the exchange of information between modelers and experimentalists.

In an even wider perspective, it might also be possible to build a unified theory that link together different type of ecosystem models, as recently proposed by Fennel and Osborn (2005) for individuals, population and biomass-based models.

Currently, the various parameters are derived from theoretical allometric considerations on the average dimension of the population or from laboratory experiments on selected single species. The high variability of natural assemblages and the difficulty of measuring the important rates of change makes the derivation of a unique set of parameters hard, especially when moving from unicellular organisms to metazoans. This is a possible limitation of this approach for the future challenge of extending the food web in order to include a detailed description of zooplankton dynamics (deYoung et al., 2004). All the CFFs are treated as bulk biomass quantities, which is an approximation that generally holds for dissolved substances and unicellular organisms. Intermediate and higher trophic levels, from small metazoans to fish, have distinct age classes and cease to behave as “functional clouds”, generally showing individual differences which results in selective feeding behaviors and a wide range of ecological strategies.

Biomass-based models, by construction, neglect the diversity of zooplankton populations. It is therefore needed to implement nesting approaches of pelagic biogeochemistry models like the one presented here with other models that are capable of simulating the functional complexity of zooplankton and fish (deYoung et al., 2004). Higher trophic levels can be key indicators of climate changes, nevertheless they are not considered in global ocean applications of pelagic biogeochemistry models. We suggest that the concepts of ecological stoichiometry can be the linkage between the different trophic levels of the global ocean ecosystem. A clear definition of the mathematical formalism used to describe the pelagic biogeochemical processes implemented in ecosystem models is thus seen as a necessary step for making this linkage effective.

Appendix

Tables with parameter description and values used in the companion paper (Vichi et al., 2006, submitted) are available as on-line supplemental material at `http://www.bo.ingv.it/~vichi/PELAGOS/tables_vichi_et_al_2006.pdf`.

Acknowledgements

We are grateful to all the members of the ERSEM team, and particularly to J.W. Baretta, H. Baretta-Bekker, W. Ebenhoeh and P. Ruardij. We wish to thank M. Zavatarelli and J.I. Allen for their helpful comments on the manuscript.

This work has been partially funded by the EU projects DYNAMITE [project no. 00393(GOCE)] for MV and SM, and MFSTEP [project no. EVK3-CT-2002-00075] for NP.

References

Allen, J., Blackford, J., Holt, J., Proctor, R., Ashworth, M., Siddorn, J., 2001. A highly spatially resolved ecosystem model for the North West European Continental Shelf. Sarsia 86, 423–440.

Allen, J., Blackford, J., Radford, P., 1998. A 1-D vertically resolved modelling study of the ecosystem dynamics of the Middle and Southern Adriatic Sea. J. Mar. Sys. 18, 265–286.

Andersen, T., Elser, J. J., Hessen, D. O., 2004. Stoichiometry and population dynamics. Ecol. Lett. 7, 884–900.

Anderson, T. R., 2005. Plankton functional type modelling: running before we can walk? J. Plankt. Res. 27, 1073–1081.

Archer, D. E., Johnson, K. S., 2000. A Model of the iron cycle in the ocean. Glob. Biogeochem. Cy. 14, 269–279.

Aumont, O., Maier-Reimer, E., Monfray, P., Blain, S., 2003. An ecosystem model of the global ocean including Fe, Si, P co-limitations. Glob. Biogeochem. Cy. 17 (2), 1060.

Baretta, J., Ebenhöh, W., Ruardij, P., 1995. The European Regional Seas Ecosystem Model, a complex marine ecosystem model. J. Sea Res. 33 (3-4), 233–246.

Baretta, J., Ruardij, P., 1988. Tidal flat estuaries: simulation and analysis of the Ems estuary. Vol. 71 of Ecol. Studies. Springer Verlag, Heidelberg.

Baretta-Bekker, J., Baretta, J., Ebenhoeh, W., 1997. Microbial dynamics in the marine ecosystem model ERSEM II with decoupled carbon assimilation and nutrient uptake. J. Sea Res. 38 (3/4), 195–212.

Baretta-Bekker, J., Baretta, J., Rasmussen, E., 1995. The microbial food web in the European Regional Seas Ecosystem Model. J. Sea Res. 33 (3-4), 363–379.

Batchelor, G., 1967. An Introduction to Fluid Dynamics. Cambridge University Press, Cambridge.

Behrenfeld, M. J., Prasil, O., Babin, M., Bruyant, F., 2004. In search of a physiological basis for covariations in light-limited and light-saturated photosynthesis. J. Phycol. 40, 4–25.

Bidle, K. D., Azam, F., 2001. Bacterial control of silicon regeneration from diatom detritus: Significance of bacterial ectohydrolases and species identity. Limnol. Oceanogr. 46 (7), 1606–1623.

Blackford, J., Radford, P., 1995. A structure and methodology for marine ecosystem modelling. J. Sea Res. 33 (3-4), 247–260.

Blackford, J. C., Allen, J. I., Gilbert, F. J., 2004. Ecosystem dynamics at six contrasting sites: a generic modelling study. J. Mar. Sys. 52, 191–215.

Blackford, J. C., Burkill, P. H., 2002. Planktonic community structure and carbon cycling in the Arabian Sea as a result of monsoonal forcing: the application of a generic model. J. Mar. Sys. 36 (3), 239–267.

Boyd, P. W., Watson, A. J., Law, C. S., Abraham, E. R., Trull, T., Murdoch, R., Bakker, D. C. E., Bowie, A. R., Buesseler, K. O., Chang, H., Charette, M., Croot, P., Downing, K., Frew, R., Gall, M., Hadfield, M., Hall, J., Harvey, M., Jameson, G., LaRoche, J., Liddicoat, M., Ling, R., Maldonado, M. T., McKay, R. M., Nodder, S., Pickmere, S., Pridmore, R., Rintoul, S., Safi, K., Sutton, P., Strzepek, R., Tanneberger, K., Turner, S., Waite, A., Zeldis, J., 2000. A mesoscale phytoplankton bloom in the polar Southern Ocean stimulated by iron fertilization. Nature 407, 695–702.

Broekhuizen, N., Heath, M., Hay, S., Gurney, W., 1995. Modelling the dynamics of the North Sea's mesozooplankton. J. Sea Res. 33 (3-4), 381–406.

Coale, K. H., Fitzwater, S. E., Gordon, R. M., Johnson, K. S., Barber, R. T., 1996. Control of community growth and export production by upwelled iron in the equatorial Pacific ocean. Nature 379, 621–624.

Denman, K. L., 2003. Modelling planktonic ecosystems: parameterizing complexity. Prog. Oceanogr. 57, 429–452.

deYoung, B., Heath, M., Werner, F., Chai, F., Megrey, B., Monfray, P., 2004. Chal-

lenges of Modeling ocean basin ecosystems. Science 304, 1463–1466.

Doney, S. C., Lindsay, K., Caldeira, K., Campin, J. M., Drange, H., Dutay, J. C., Follows, M., Gao, Y., Gnanadesikan, A., Gruber, N., Ishida, A., Joos, F., Madec, G., Maier-reimer, E., Marshall, J. C., Matear, R. J., Monfray, P., Mouchet, A., Najjar, R., Orr, J. C., Plattner, G. K., Sarmiento, J., Schlitzer, R., Slater, R., Totterdell, I. J., Weirig, M. F., Yamanaka, Y., Yool, A., 2004. Evaluating global ocean carbon models: The importance of realistic physics. Glob. Biogeochem. Cy. 18, 3017.

Ebenhöh, W., Baretta-Bekker, J., Baretta, J., 1997. The primary production module in the marine ecosystem model ERSEM II with emphasis on the light forcing. J. Sea Res. 38, 173–193.

Elser, J. J., Hessen, D. O., 2005. Biosimplicity via stoichiometry: the evolution of food-web structure and processes. In: A. Belgrano, Scharler, D., Ulanowicz, U. (Eds.), Aquatic Food Webs: an Ecosystem Approach. Oxford University Press, Oxford, UK, pp. 7–18.

Fennel, W., Osborn, T., 2005. A unifying framework for marine ecological model comparison. Deep-Sea Res. Pt. II 52, 1344–1357.

Flynn, K. J., 2001. A mechanistic model for describing dynamic multi-nutrient, light, temperature interactions in phytoplankton. J. Plankt. Res. 23, 977–997.

Flynn, K. J., Marshall, H., Geider, R. J., 2001. A comparison of two N-irradiance interaction models of phytoplankton growth. Limnol. Oceanogr. 46, 1794–1802.

Frost, P. C., Xenopoulos, M. A., Larson, J. H., 2004. The stoichiometry of dissolved organic carbon, nitrogen, and phosphorus release by a planktonic grazer, Daphnia. Limnol. Oceanogr. 49, 1802–1808.

Fung, I. Y., Meyn, S. K., Tegen, I., Doney, S. C., John, J. G., Bishop, J. K. B., 2000. Iron supply and demand in the upper ocean. Glob. Biogeochem. Cy. 14, 281–295.

Geider, R., MacIntyre, H., Kana, T., 1996. A dynamic model of photoadaptation in phytoplankton. Limnol. Oceanogr. 41 (1), 1–15.

Geider, R., MacIntyre, H., Kana, T., 1997. A dynamic model of phytoplankton growth and acclimation: responses of the balanced growth rate and chlorophyll *a*:carbon ratio to light, nutrient limitation and temperature. Mar. Ecol. Prog. Ser. 148, 187–200.

Geider, R., MacIntyre, H., Kana, T., 1998. A dynamic regulatory model of phytoplanktonic acclimation to light, nutrients, and temperature. Limnol. Oceanogr. 43 (3), 679–694.

Gentleman, W., Leising, A., Frost, B., Strom, S., Murray, J., 2003. Functional responses for zooplankton feeding on multiple resources: a review of assumptions and biological dynamics. Deep-Sea Res. Pt. II 50, 2847–2875.

Gibson, G. A., Musgrave, D. L., Hinckley, S., 2005. Non-linear dynamics of a pelagic ecosystem model with multiple predator and prey types. J. Plankt. Res. 27, 427–447.

Ho, T. Y., Quigg, A., Finkel, Z. V., Milligan, A. J., Wyman, K., Falkowski, P. G., Morel, F. M. M., 2003. The elemental composition of some marine phytoplankton. J. Phycol. 39, 1145–1159.

Hofmann, E., Lascara, C., 1998. Overview of Interdisciplinary Modeling for Marine Ecosystems. In: Brink, K. H., Robinson, A. R. (Eds.), The Sea. Vol. 10. John Wiley & Sons, Inc., New York, pp. 507–540.

Johnson, K. S., Gordon, R. M., Coale, K. H., 1997. What controls dissolved iron concentrations in the world ocean? Mar. Chem. 57, 137–161.

Kraemer, S. M., 2004. Iron oxide dissolution and solubility in the presence of siderophores. Aquat. Sci. 66, 3–18.

Le Quéré, C., Harrison, S., Prentice, I., Buitenhuis, E., Aumont, O., Bopp, L., Claustre, H., da Cunha, L. C., Geider, R., Giraud, X., Klaas, C., Kohfeld, K., Legendre, L., Manizza, M., Platt, T., Rivkin, R., Sathyendranath, S., Uitz, J., Watson, A., Wolf-Gladrow, D., 2005. Ecosystem dynamics based on plankton functional types for global ocean biogeochemistry models. Glob. Change Biol. 11, 2016–2040.

Lefevre, N., Watson, A. J., 1999. Modeling the geochemical cycle of iron in the oceans and its impact on atmospheric CO2 concentrations. Global Biogeochem Cy 13, 727–736.

Leonard, C. L., Mcclain, C. R., Murtugudde, R., Hofmann, E. E., Harding, L. W., 1999. An iron-based ecosystem model of the central equatorial pacific. J. Geophys. Res. 104, 1325–1341.

Martin, J. H., Coale, K. H., Johnson, K. S., Fitzwater, S. E., Gordon, R. M., Tanner, S. J., Hunter, C. N., Elrod, V. A., Nowicki, J. L., Coley, T. L., Barber, R. T., Lindley, S., Watson, A. J., Vanscoy, K., Law, C. S., Liddicoat, M. I., Ling, R., Stanton, T., Stockel, J., Collins, C., Anderson, A., Bidigare, R., Ondrusek, M., Latasa, M., Millero, F. J., Lee, K., Yao, W., Zhang, J. Z., Friederich, G., Sakamoto, C., Chavez, F., Buck, K., Kolber, Z., Greene, R., Falkowski, P., Chisholm, S. W., Hoge, F., Swift, R., Yungel, J., Turner, S., Nightingale, P., Hatton, A., Liss, P., Tindale, N. W., 1994. Testing the iron hypothesis in ecosystems of the equatorial Pacific Ocean. Nature 371, 123–129.

Martin, J. H., Gordon, R. M., Fitzwater, S. E., 1991. The case for iron. Limnol. Oceanogr. 36, 1793–1802.

McCarthy, J., Robinson, A., Rothschild, B., 2002. Biological-physical interactions in the sea: Emergent findings and new directions. In: Robinson, A., McCarthy, J., Rothschild, B. (Eds.), The Sea. Vol. 12. John Wiley & Sons, Inc., New York, Ch. 1, pp. 1–17.

Mitra, A., Flynn, K. J., 2005. Predator-prey interactions: is 'ecological stoichiometry' sufficient when good food goes bad? J. Plankt. Res. 27, 393–399.

Obernosterer, I., Ruardij, P., Herndl, G., 2001. Spatial and diurnal dynamics of dissolved organic matter (DOM) fluorescence and H_2O_2 and the photochemical oxygen demand of surface water DOM across the subtropical Atlantic Ocean. Lymnol. Oceanogr. 46 (3), 632–643.

Ogawa, H., Tanoue, E., 2003. Dissolved organic matter in oceanic waters. J. Oceanogr. 59, 129–147.

Olsen, A., Wanninkhof, R., Trinanes, J. A., Johannessen, T., 2005. The effect of wind speed products and wind speed-gas exchange relationships on interannual variability of the air-sea CO2 gas transfer velocity. Tellus B 57, 95–106.

Parekh, P., Follows, M. J., Boyle, E., 2004. Modeling the global ocean iron cycle. Glob. Biogeochem. Cy. 18, GB1002.

Petihakis, G., Triantafyllou, G., Allen, I. J., Hoteit, I., Dounas, C., 2002. Modelling the spatial and temporal variability of the Cretan Sea ecosystem. J. Mar. Sys. 36, 173–196.

Platt, T., Gallegos, C. L., Harrison, W. G., 1980. Photoinhibition of photosynthesis in natural assemblages of marine phytoplankton. J. Mar. Res. 38, 687–701.

Polimene, L., Allen, J. I., Zavatarelli, M., 2006. Dissolved Organic Carbon-bacteria interactions in marine systems: a theoretical modelling study, in press.

Price, N. M., 2005. The elemental stoichiometry and composition of an iron-limited diatom. Limnol. Oceanogr. 50, 1159–1171.

Raick, C., Delhez, E. J. M., Soetaert, K., Gregoire, M., 2005. Study of the seasonal cycle of the biogeochemical processes in the Ligurian Sea using a ID interdisciplinary model. J. Mar. Sys. 55, 177–203.

Reinart, A., Arst, H., Blanco-Sequeiros, A., Herlevi, A., 1998. Relation between underwater irradiance and quantum irradiance in dependence on water transparency at different depths in the water bodies. J. Geophys. Res. 103 (C4), 7759–7752.

Ruardij, P., Haren, H. V., Ridderinkhof, H., 1997. The impact of thermal stratification on phytoplankton and nutrient dynamics in shelf seas: a model study. J. Sea Res. 38 (3-4), 311–331.

Ruardij, P., Van Raaphorst, W., 1995. Benthic nutrient regeneration in the ERSEM ecosystem model of the North Sea. J. Sea Res. 33 (3-4), 453–483.

Sakshaug, E., Bricaud, A., Dandonneau, Y., Falkowski, P. G., Kiefer, D. A., Legendre, L., Morel, A., Parslow, J., Takahashi, M., 1997. Parameters of photosynthesis: definitions, theory and interpretation of results. J. Plankt. Res. 19, 1637–1670.

Schmidt, M. A., Zhang, Y. H., Hutchins, D. A., 1999. Assimilation of Fe and carbon by marine copepods from Fe-limited and Fe-replete diatom prey. J. Plankt. Res. 21, 1753–1764.

Smith, T., Shugart, H. H., Woodward, F. I., 1997. Plant functional types: their relevance to ecosystem properties and climate change. Cambridge University Press, Cambridge.

Sterner, R. W., Elser, J. J., 2002. Ecological stoichiometry: the biology of elements from molecules to the biosphere. Princeton University Press, Princeton, NJ.

Strzepek, R. F., Harrison, P. J., 2004. Photosynthetic architecture differs in coastal and oceanic diatoms. Nature 431, 689–692.

Sunda, W. G., 1997. Control of dissolved iron concentrations in the world ocean: A comment. Mar. Chem. 57, 169–172.

Sunda, W. G., Huntsman, S. A., 1995. Iron uptake and growth limitation in oceanic and coastal phytoplankton. Mar. Chem. 50, 189–206.

Sunda, W. G., Huntsman, S. A., 1997. Interrelated influence of iron, light and cell size on marine phytoplankton growth. Nature 390, 389–392.

Taylor, A. H., Allen, J. I., Clark, P. A., 2002. Extraction of a weak climatic signal by an ecosystem. Nature 416, 629–632.

Timmermans, K. R., van der Wagt, B., de Baar, H. J. W., 2004. Growth rates, half-saturation constants, and silicate, nitrate, and phosphate depletion in relation to iron availability of four large, open-ocean diatoms from the Southern ocean. Limnol. Oceanogr. 49, 2141–2151.

Timmermans, K. R., van der Wagt, B., Veldhuis, M. J. W., Maatman, A., de Baar, H. J. W., 2005. Physiological responses of three species of marine pico-phytoplankton to ammonium, phosphate, iron and light limitation. J. Sea Res. 53, 109–120.

Varela, R., Cruzado, A., Gabaldon, J., 1995. Modelling primary production in the North Sea using the European Regional Seas Ecosystem Model. J. Sea Res. 33 (3-4), 337–361.

Vichi, M., 2002. Predictability studies of coastal marine ecosystem behavior. Ph.D. thesis, University of Oldenburg, Oldenburg, Germany.
URL http://docserver.bis.uni-oldenburg.de/publikationen/dissertation/2002/vicpre02/vicpre02.html

Vichi, M., Masina, S., Navarra, A., 2006. A generalized model of pelagic biogeochemistry for the global ocean ecosystem. Part II: numerical simulations. J. Mar. Sys. XX, xxx–xxx, in press.

Vichi, M., May, W., Navarra, A., 2003a. Response of a complex ecosystem model of the northern Adriatic Sea to a regional climate change scenario. Climate Research 24, 141–159.

Vichi, M., Oddo, P., Zavatarelli, M., Coluccelli, A., Coppini, G., Celio, M., Fonda Umani, S., Pinardi, N., 2003b. Calibration and validation of a one-dimensional complex marine biogeochemical fluxes model in different areas of the northern Adriatic shelf. Ann. Geophys. 21, 413–436.

Vichi, M., Ruardij, P., Baretta, J. W., 2004. Link or sink: a modelling interpretation of the open Baltic biogeochemistry. Biogeosciences 1, 79–100.

Vichi, M., Zavatarelli, M., Pinardi, N., 1998. Seasonal modulation of microbial-mediated carbon fluxes in the Northern Adriatic Sea. Fisheries Oceanography 7 (3/4), 182–190.

Webb, W., Newton, M., Starr, D., 1974. Carbon dioxide exchange of *alnus rubra*: a mathematical model. Ecologia 17, 281–291.

Worden, A. Z., Nolan, J. K., Palenik, B., 2004. Assessing the dynamics and ecology of marine picophytoplankton: The importance of the eukaryotic component. Limnol. Oceanogr. 49, 168–179.

Zavatarelli, M., Baretta, J., Baretta-Bekker, J., Pinardi, N., 2000. The dynamics of the Adriatic Sea ecosystem; an idealized model study. Deep-Sea Res. Pt. I 47, 937–970.

Zeebe, R. E., Wolf-Gladrow, D. A., 2001. CO_2 in Seawater: Equilibrium, Kinetics, Isotopes. Vol. 65 of Oceanography Book Series. Elsevier, Amsterdam.

Variable	Type	Components	# of CFFs	Description	Reference
$N^{(1)}$	IO	P	1	Phosphate (mmol P m^{-3})	Baretta et al., 1995
$N^{(3)}$	IO	N	1	Nitrate (mmol N m^{-3})	"
$N^{(4)}$	IO	N	1	Ammonium (mmol N m^{-3})	"
$N^{(5)}$	IO	Si	1	Silicate (mmol Si m^{-3})	"
$N^{(6)}$	IO	R	1	Reduction equivalents, HS^- (mmol S m^{-3})	Vichi et al., 2004;
$N^{(7)}$	IO	Fe	1	Dissolved iron (μmol Fe m^{-3})	this work;
$O^{(2)}$	IO	O	1	Dissolved Oxygen (mmol O_2 m^{-3})	Baretta et al., 1995;
$O^{(3)}$	IO	C	1	Carbon Dioxide (mg C m^{-3})	-
$P_i^{(1)}$	LO	C N P Si Fe Chl	6	Diatoms (mg C m^{-3}, mmol N-P-Si m^{-3}, μmol Fe m^{-3} and mg Chl-*a* m^{-3})	Varela et al., 1995; Ebenhoeh et al., 1997; Baretta-Bekker et al., 1997; this work
$P_i^{(2)}$	LO	C N P Fe Chl	5	Flagellates (")	"
$P_i^{(3)}$	LO	C N P Fe Chl	5	Picophytoplankton (")	"
B_i	LO	C N P	3	Pelagic Bacteria (")	Baretta-Bekker et al., 1995; Baretta-Bekker et al., 1997
$Z_i^{(4)}$	LO	C N P	3	Omnivorous Mesozooplankton (")	Broekhuizen et al., 1995; this work
$Z_i^{(5)}$	LO	C N P	3	Microzooplankton (")	Baretta-Bekker et al., 1995, 1997; this work
$Z_i^{(6)}$	LO	C N P	3	Heterotrophic Flagellates (")	"
$R_i^{(1)}$	NO	C N P	3	Dissolved Organic Detritus (")	Baretta et al., 1995; Vichi et al., 2003a
$R_i^{(6)}$	NO	C N P Si Fe	5	Particulate Organic Detritus (")	"

Table 1
List of the Chemical Functional Family state variables (CFF, for a total of 44 prognostic equations) for the pelagic model and references to the original publications. Type legend: IO = Inorganic; LO = Living organic; NO = Non-living organic. The subscript i indicates the basic components (if any) of the CFF, e.g. $P_i^{(1)} \equiv \left(P_c^{(1)}, P_n^{(1)}, P_p^{(1)}, P_s^{(1)}, P_l^{(1)}, P_f^{(1)}\right)$.

Abbreviation	**Comment**
gpp	Gross primary production
rsp	Respiration
prd	Predation
rel	Biological release: Egestion, Excretion
exu	Exudation
lys	Lysis
syn	Biochemical synthesis
nit/denit	Nitrification, denitrification
scv	Scavenging
rmn	Biochemical remineralization
upt	Uptake

Table 2
List of all the abbreviations used to indicate the physiological and ecological processes in (5).

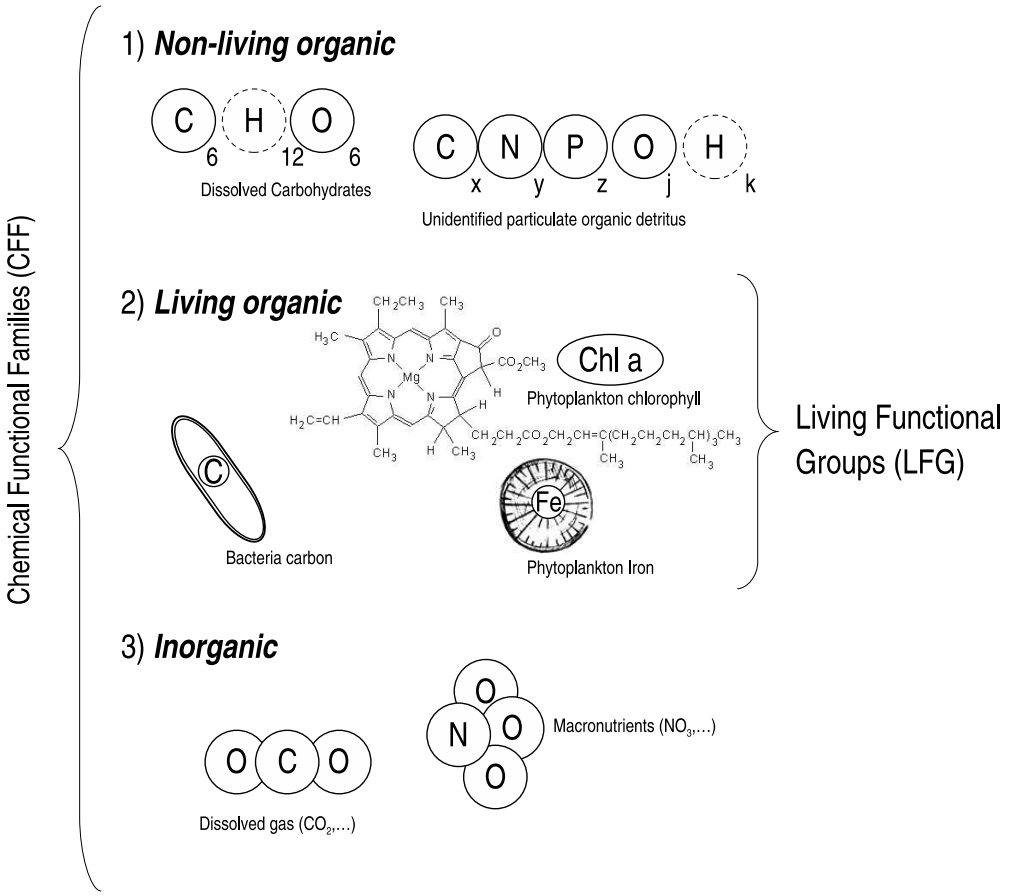

Figure 1. Scheme of the various types of Chemical Functional Families (CFF) expressed in terms of basic biogeochemical elements. Hidrogen is not considered a basic constituent in the model but is indicated for completeness of the chemical compound formulations. Living organic CFFs are the basis for the modelling of Living Functional Groups (LFGs).

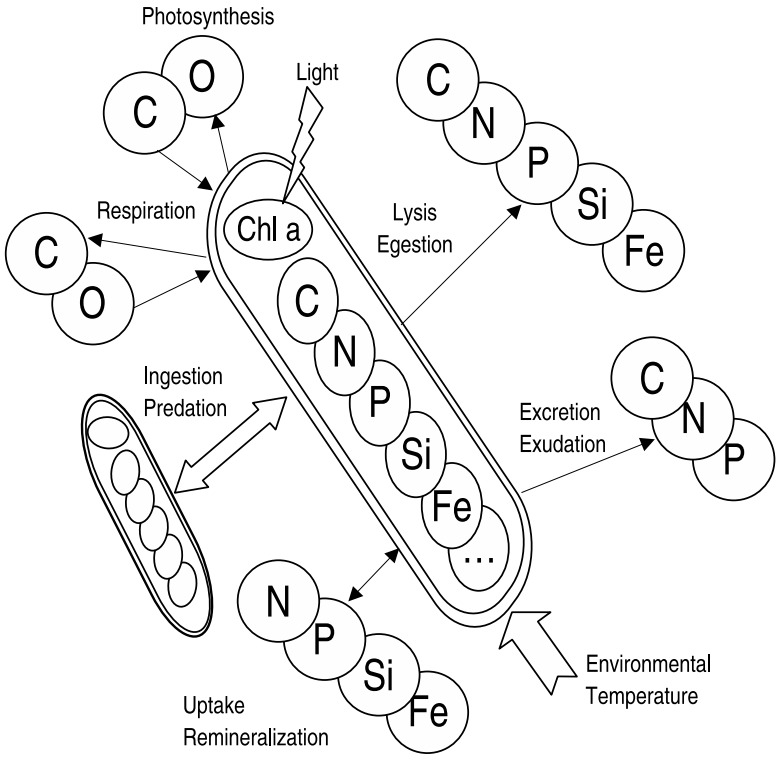

Figure 2. Scheme of the standard organism, which is the prototype of any Living Functional Group (LFG), and the physiological/trophic relationships among the Chemical Functional Families and major environmental forcings. The standard organism is a theoretical representation of the real organisms and can describe both an autotroph, a heterotroph or a mixotroph, depending on the choice of the (internal) living CFFs and the process equations that link them.

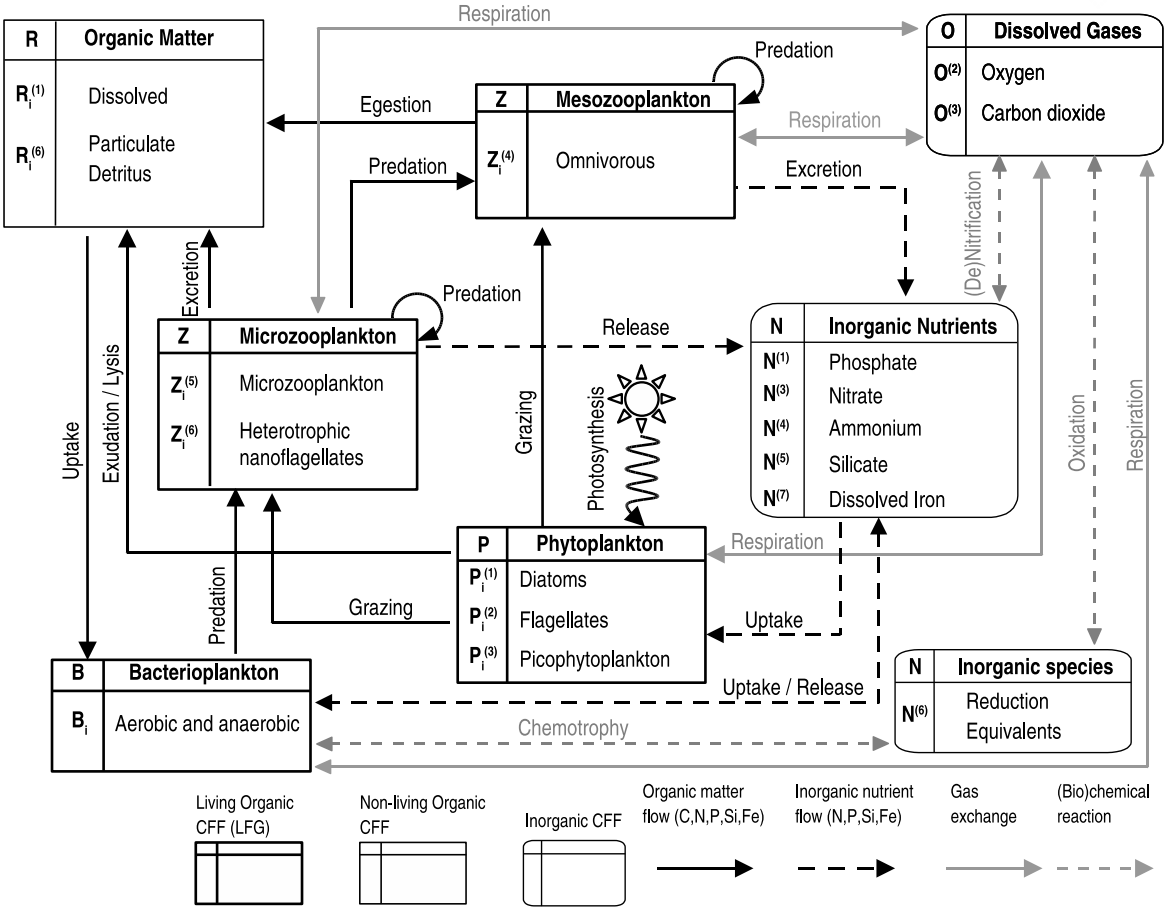

Figure 3. Scheme of the state variables and pelagic interactions of the biogeochemistry model. Living (organic) Chemical Functional Families (CFF) are indicated with bold-line square boxes, non-living organic CFFs with thin-line square boxes and inorganic CFFs with rounded boxes (modified after Blackford and Radford (1995)).